

Master's Thesis
석사 학위논문

Study of Nano-structure Coupling Micro-Scale
Antenna for Signal and Power Transmission using
Magnetic Induction to an Implanted Device in the
Human Body

Jong-Gu Kang (강 종 구 姜 鍾 求)

Department of Information and Communication Engineering

정보통신융합공학전공

DGIST

2014

Master's Thesis
석사 학위논문

Study of Nano-structure Coupling Micro-Scale
Antenna for Signal and Power Transmission using
Magnetic Induction to an Implanted Device in the
Human Body

Jong-Gu Kang (강 종 구 姜 鍾 求)

Department of Information and Communication Engineering

정보통신융합공학전공

DGIST

2014

Study of Nano-structure Coupling Micro-Scale An-tenna for Signal
and Power Transmission using Magnetic Induction to an Implanted
Device in the Human Body

Advisor : Professor Jae Eun Jang

Co-advisor : Professor Jung-II Hong

By

Jong-Gu Kang

Department of Information and Communication Engineering
DGIST

A thesis submitted to the faculty of DGIST in partial fulfillment of the requirements for the degree of Master of Science in the Department of Information and Communication Engineering. The study was conducted in accordance with Code of Research Ethics¹

12(month). 23(day). 2013(year)

Approved by

Professor 장재은 (Signature)
(Advisor)

Professor 홍정일 (Signature)
(Co-Advisor)

¹ Declaration of Ethical Conduct in Research: I, as a graduate student of DGIST, hereby declare that I have not committed any acts that may damage the credibility of my research. These include, but are not limited to: falsification, thesis written by someone else, distortion of research findings or plagiarism. I affirm that my thesis contains honest conclusions based on my own careful research under the guidance of my thesis advisor.

Study of Nano-structure Coupling Micro- Scale Antenna for a Signal
and Power Transmission Using Magnetic Induction to an
Implanted Device in the Human Body

Jong-Gu Kang

Accepted in partial fulfillment of the requirements for the degree of Master of
Science.

12(month). 23(day). 2013(year)

Head of Committee 장 재 은 (인)

Prof. Jae Eun Jang

Committee Member 홍 정 일 (인)

Prof. Jung-Il Hong

Committee Member 최 지 응 (인)

Prof. Ji-Woong Choi

MS/IC
201222001

강 종 구. Jong-Gu Kang. Study of Nano-structure Coupling Micro-Scale Antenna for Signal and Power Transmission using Magnetic Induction to an Implanted Device in the Human Body, Department of Information and Communication engineering. 2013. 59p. Advisors Prof. Jae Eun Jang, Prof. Co-Advisors Prof. Jung-II Hong.

ABSTRACT

Currently, communication systems using radio frequency (RF) are the mainstream of functional devices. In the case of wireless communication devices such as mobile phones, tablet PCs, and medical devices, they can transmit an electrical signal from one device to another without a wire connection. However, this technology is not suitable for the power transmission due to limitations such as low power efficiency and noise caused by interference from outside objects. Furthermore, the path loss is more severe when RF technology is applied to power transmission between an implanted human sensory system and external interfaces to transfer power, since 80 % of the human body is composed of water molecules. To overcome these limitations, this study focuses on magnetic induction (MI) system, which uses magnetic coupling of a pair of coils to transmit signals and power between devices. For magnetic fields, the path loss of water or other liquid media is smaller than that of RF waves. So far, most research results related with magnetic induction system have shown power transmission using macro-size coil structures. However, medical implant devices have the limit of the physical dimensions which requires the coil structure as small as possible. Unfortunately, a micro-size antenna can have poor transmittance efficiency due to its size effect. Therefore, micro-size antennas with advanced structures should be investigated to overcome these challenges. This paper describes the coil designs and the characteristics of power transmission between a transmitter (Tx) and a receiver (Rx). To enhance the magnetic inductance, a three dimensional magnetic core consisted of ZnO nano wires coated by a nickel (Ni) layer is added to the center of antenna structure. ZnO nano wires easily supply a large effective surface area with a vertical structural effect to the magnetic core structure, which induces a higher magnetic inductance with a ferro-magnetic material Ni. The magnetic induction coil with the magnetic core shows a high inductance value, a low reflection power and a strong power transmission.

Keywords: Magnetic Induction, Magnetic core, Nano wire

List of contents

Abstract	i
List of contents	ii
List of tables	iv
List of figures	v

I . INTRODUCTION

1.1 Motivation	1
1.2 History of power transmission	2
1.3 Background principles of wireless power transmission	5
1.3.1 Radio frequency (RF) system	5
1.3.2 Magnetic Induction (MI) system	6
1.3.3 Magnetic Resonance (MR) system	7
1.4 Theory of magnetic field	9
1.5 Antenna structure for power transmission	10
1.5.1 Coil design	10
1.5.2 Magnetic core (MC) structure	13

II . EXPERIMENT DETAILS

2.1 Fabrication of the basic coil	16
2.2 Designing magnetic core (MC) structure	19
2.3 Experiment condition	20

III. RESULTS AND DISCUSSION

3.1 Results of micro size antennas for the magnetic induction (MI)	22
3.2 Electrical characteristics of basic coils	25
3.2.1 Theoretical values of an inductance	25
3.2.2 Measurement values of resistances and inductances	27
3.2.3 Measurement values of a self-resonant frequency	29

3.3 Electrical characteristics of magnetic core (MC) coils	32
3.4 Power transmission	37
3.4.1 In the air	37
3.4.2 In the water	38
3.4.3 The effect of matching a resonant frequency and impedance	39
3.4.4 The effect of the power transmission over changing frequencies	41
3.4.5 Matching a resonant frequency at Rx	42
IV. CONCLUSION	44

List of tables

Table I. Comparison of Single and Double layers	13
Table II. DC resistance of the theoretical and I-V characterization system	26
Table III. The theoretical and measured inductance values	27

List of figures

Figure 1.1.1 The field of wireless applications	2
Figure 1.2.1 The mechanism of Faraday's and Ampere's law	4
Figure 1.3.1 The mechanism of Radio Frequency (RF)	6
Figure 1.3.2 The mechanism of magnetic induction (MI) method.....	7
Figure 1.3.3 The mechanism of magnetic resonance (MR) method	8
Figure 1.3.4 Comparison of experimental and theoretical values for k	8
Figure 1.4.1 The cross sectional view of magnetic field created by a solenoid	10
Figure 1.5.1 Various types of a coil	11
Figure 1.5.2 Comparison of the results the 3D FE simulations for magnetic coupling k	11
Figure 1.5.3 Parameters of a single layer on the ferrite layer and no ferrite layer	14
Figure 1.5.4 The influence of magnetic core (MC) in the coil	15
Figure 2.1.1 The design of 4 inch wafer for various coils	16
Figure 2.1.2 The process of photolithography and growing ZnO nano wires – Ni layer	18
Figure 2.2.1 The process of growing ZnO nano wires	20
Figure 2.3.1 The experiment condition	21
Figure 3.1.1 Optical images and scanning electron microscope (SEM) images	23
Figure 3.1.2 The SEM images of a boundary between a width and spacing ..	24
Figure 3.2.1 The inductance values of coils with various diameter and turns ..	29
Figure 3.2.2 The electrical characteristics of basic flat spiral antennas	30~31
Figure 3.3.1 The flat spiral antenna structure with magnetic core (MC) consisting of ZnO nano wires and Ni layer	33
Figure 3.3.2 The data of ZnO nano wires in XRD and PL	34
Figure 3.3.3 Electrical characteristics of 1 mm 1turn antenna structure with the MC and without the MC	35
Figure 3.3.4 The inductance values under an outer diameter (1mm) with MC and without MC	36

Figure 3.4.1 The power transmission in the air	37
Figure 3.4.2 The power transmission in the water	39
Figure 3.4.3 The matching effect of a resonant frequency and impedance	40
Figure 3.4.4 The effect of the power transmission over changing frequencies	41
Figure 3.4.5 The matching effect of a resonant frequency at Rx	43

I. INTRODUCTION

1.1 Motivation

Currently, the power transmission system in human implanted devices is the mainstream [1]. Electrical devices such as an artificial cochlear, an artificial retina or medical sensors, these electrical devices need a power system to supply stable energy [2][3][4]. For a long time, engineers have developed power systems which include a battery and wire connection between the inside and the outside. In the case of these two main systems, there are limitations. One issue is the charging problem. It is necessary to plug implanted devices into an outlet in order to charge them. This plug-in electrical circuit makes unnecessary power consumption, constraints of space and a complicated design. The other limitation is environment. Generally, batteries are made from a chemical processes that contains acidic or alkaline chemicals, heavy metals, lithium and cadmium. Those extreme toxins can cause severe damage to the human implanted devices [1]. Also, a laparotomy is required to change the battery. Wire connections and batteries are inconvenient and hazardous, whereas wireless power transmission is more suitable.

This wireless power transmission technique is the transmission of the power source from transmitter (Tx) to receiver (Rx) without any wire power cables and can be supplied continuously from external energy source. It is more comfortable, safer and uses less space than wired power systems. Figure 1.1.1 shows the field of wireless applications [5]. The method of a wireless power transmission is divided into three mechanisms which are magnetic induction (MI), magnetic resonance (MR) and radio frequency (RF). An industry robot, radio frequency identification (RFID) and electric toothbrush are on MI

method. A vacuum, television (TV), mobile phone, and implanted devices are on the MR or MI field. The space solar light power and sensor are on the radio frequency (RF) area.

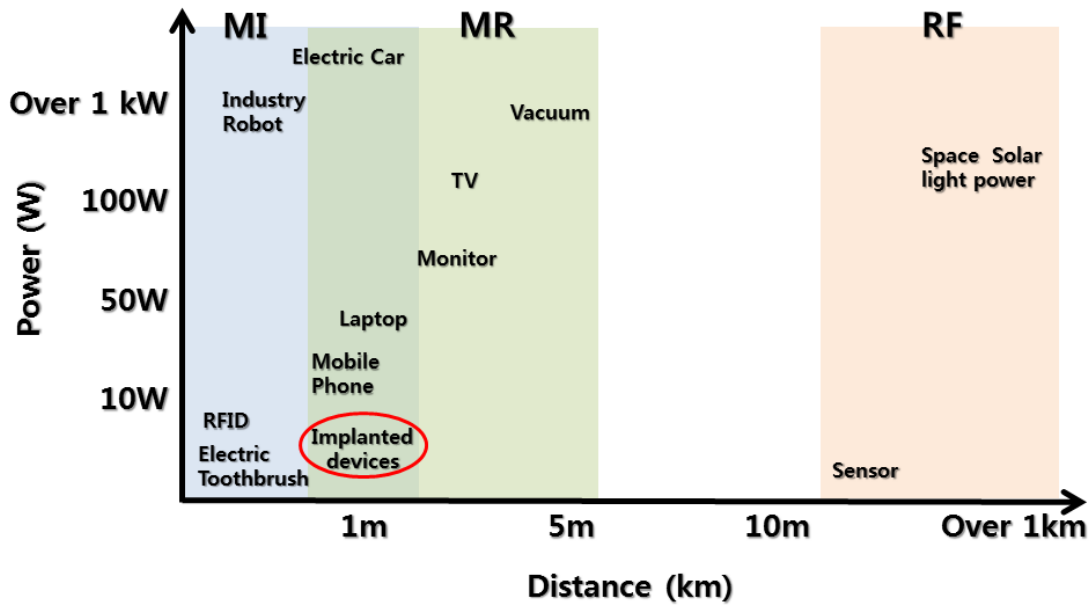


Fig 1.1.1 The field of wireless applications [5]

The human implanted devices located on the boundary between magnetic induction (MI) and magnetic resonance (MR). The cover range is around 1 m and the operated power is under 10 Watt (W). This means that the human implanted devices need to research both MI and MR mechanism to optimize wireless power transmission.

1.2 History of Power Transmission

The quality of life has been improved by inventing electric power. The human can work at night like in the daytime. Also, a washing machine, vacuum cleaner and communication machines have been used since the electric power was invented. However, the human live under various cables such as power cables, telephone cables, internet ca-

bles and antenna cables. These cables can be seen around our life and cause inconvenient problems for example a wasting space and a material consumption. To overcome these inconvenient problems, various methods have been researched for a long time.

Andre Marie Ampere who was a French physicist and mathematician developed Ampere's law in the early 19th century [6]. This law shows that a time varying electrical current produces a time varying magnetic field and is a good predictor of the existence of propagating electromagnetic waves. After presenting Ampere's law, Michael Faraday, who was an English scientist, contributed the fields of electromagnetic induction [6]. In 1831, he developed Faraday's law of induction describing the electromagnetic force induced in a conductor by a time varying magnetic flux. These two theories are the fundamental mechanisms to support wireless power transmission. Nikola Tesla who was 20th century inventor conceived various induction machines such as fans, pumps, air-conditioning systems, electric vehicles and electric railway systems [6][7]. In his achievements, wireless power transmission with radiative and tunable characteristics has been focused on by a large number of engineers and scientists due to its low efficiency and radiative loss due to its omnidirectional nature.

$$\begin{aligned}\nabla \times \mathbf{E} &= -\frac{\partial \mathbf{B}}{\partial t} \\ \nabla \times \mathbf{H} &= \mathbf{J} + \frac{\partial \mathbf{D}}{\partial t} \\ \nabla \cdot \mathbf{D} &= \rho \\ \nabla \cdot \mathbf{B} &= 0\end{aligned}\tag{1} [6]$$

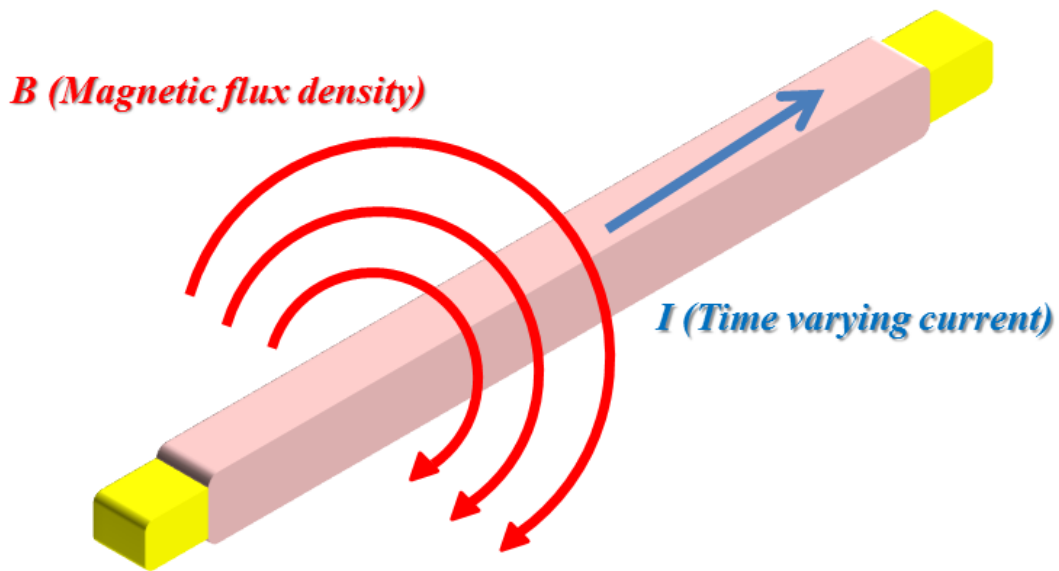


Fig 1.2.1 The mechanism of Faraday's and Ampere's law

Equation 1 is presented in Maxwell's equations [6]. The first is Faraday's law. This expression includes ' E ' and ' B ' which are an electric field and magnetic flux density. When being varying magnetic fields around a conducting wire, time varying electric fields are flowed in the conducting wire. This is a power source to operate electric devices. Second equation shows Ampere's law. There are ' H ', ' J ' and ' D ', each quantities are magnetic field intensity, an electric current density and electric flux density. When applying time varying current in a conducting wire, time varying magnetic field propagated in a channel around the conducting wire. Figure 1.2.1 shows the mechanism of faraday's and Ampere's law. One of the latest wireless power transmissions was MIT's wireless power transfer which was published in the year 2007 and was titled "Wireless Power Transfer via Strongly Coupled Magnetic Resonances." [8] The concept behind their research is two self-resonant coils located in the channel. One coil (the source coil) is coupled inductively to an oscillating circuit; the other (the device coil) is coupled inductively

to a resistive load. Self-resonant coils rely on the interplay between distributed inductance and distributed capacitance to achieve resonance.

1.3 Background principles of wireless power transmission

1.3.1 Radio frequency (RF) system

A radio frequency (RF) system mainly propagates electromagnetic waves in a channel in Fig 1.3.1. The mechanism uses the electromagnetic waves from transmitter (Tx), the rectenna consisting of an antenna and a rectifier that receives the electromagnetic waves. The system then transfers the electromagnetic waves into a power source to operate electric devices [9][10][11]. This technique is useful to miniature sensors such as temperature and humidity sensors that require low power consumption. Mobile communication is a representative application. RF systems make it possible to transfer several dozens of kilowatts (kw) dozens to the Rx over several dozens of kilometers (km). This technique has been studied for space solar power system (SSPS) or as an alternative of a power transmission tower. The national aeronautics and space administration (NASA), in 1970, has already succeeded in transmitting 30 kilowatts power to a receiver (Rx) over a distance of approximately 1.4 km. However, in this RF system, most propagated electromagnetic waves are lost during the transmission process in the channel and are harmful to human health because the RF radiates energy from both magnetic waves and electric waves in the channel. In addition, in order to satisfy the regulation of electromagnetic waves, the maximum power limitation is about 1 kw. This small amount is insufficient to charge portable electrical devices.

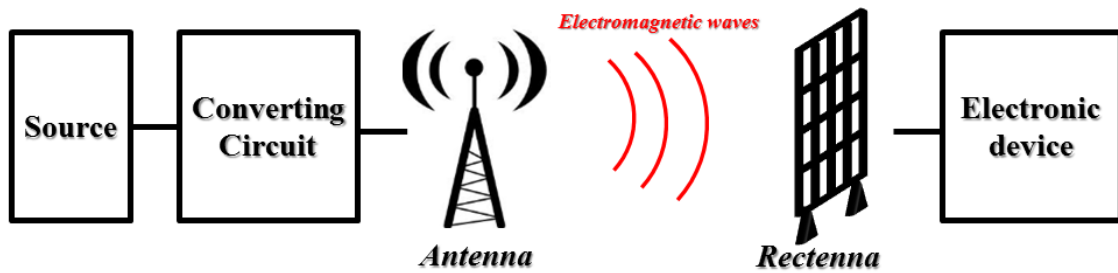


Fig 1.3.1 The mechanism of Radio Frequency (RF) method

1.3.2 Magnetic induction (MI) system

The Magnetic induction (MI) technique has already been used by commercial motors and transformer since 1800 [9][12]. The main working principle involves a Tx antenna and Rx antenna coupled by magnetic flux through both coils. Specifically, the time varying current in the Tx coil generates a magnetic field which induces voltage in the Rx coil in Fig 1.3.2. This induced voltage can be a power source to operate electrical devices. Recently, this MI technique has been applied to electric toothbrushes, radio frequency identification (RFID), cell phone battery chargers and electric automobiles. While the efficiency of power transmission is over 90%, but this MI technique has a limited working area of just several millimeters (mm). Also, if both the Tx coil and the Rx coil are not aligned exactly, the efficiency of power transmission is poor. In addition, the MI technique needs both the coils to be aligned horizontally to get high efficiency power transmission. So, this power transmission is closer to a wire connection. However, there is a strong point that MI method is accepted by an international standardization. It is not harmful to a human body.

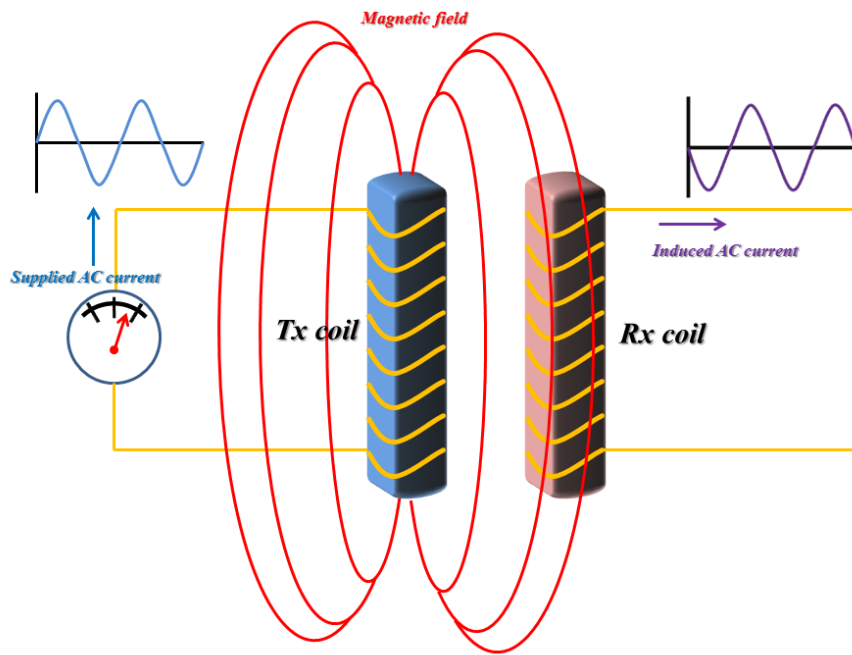


Fig 1.3.2 The mechanism of magnetic induction (MI) method

1.3.3 Magnetic resonance (MR) system.

The magnetic resonance (MR) system was devised by a Massachusetts Institute of Technology (MIT) research team in 2007 [8]. This MR technique was created based on the concept of a tuning fork. Once one tuning fork is stricken among various turning forks with different natural frequencies, the other turning fork with the same nature frequency vibrates. This physical phenomenon is called to resonance. Like this fundamental theory, in the MR system the Rx is designed by a certain frequency and receives power from a magnetic field generated by a Tx with the same resonant frequency. The coils are made of an electrically conducting wire of a total length of ' l ' and a cross section radius of ' a ' wound into a helix of ' n ' turns, radius ' r ', and height ' h '. They succeeded in demonstrating the ability of magnetically coupled coils to transfer power wirelessly over a short distance.

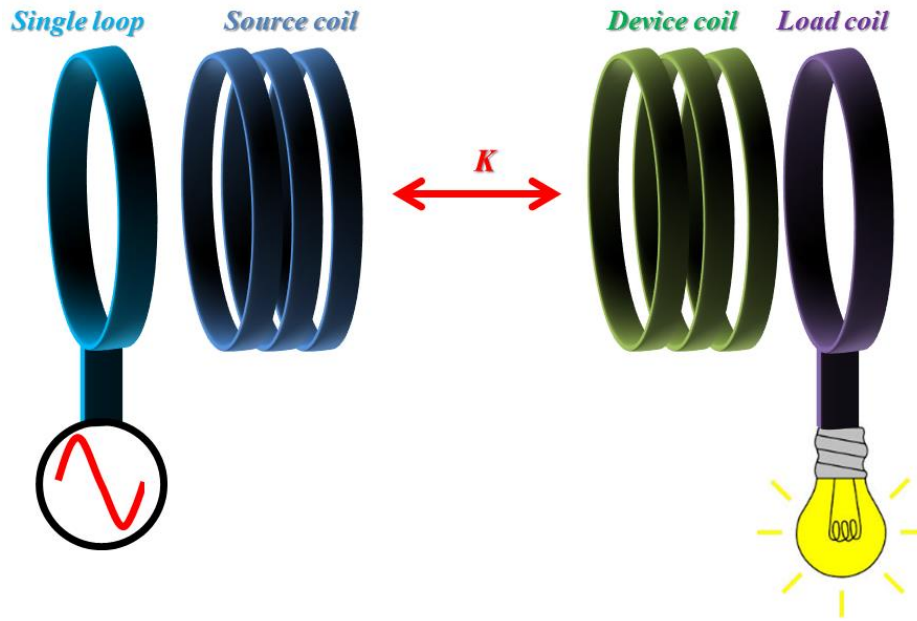


Fig 1.3.3 The mechanism of magnetic resonance (MR) method [8]

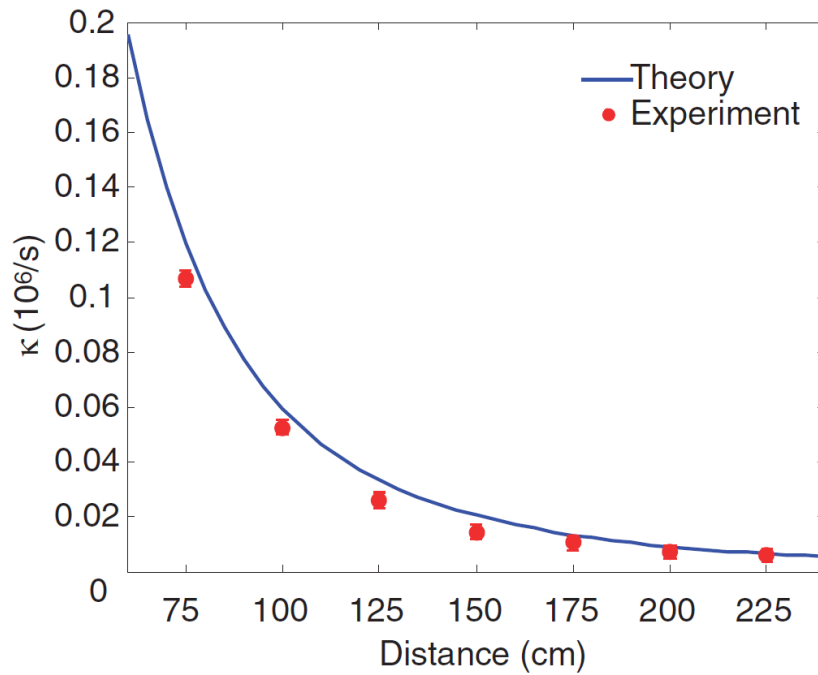


Fig 1.3.4 Comparison of experimental and theoretical values for K [8]

Figure 1.3.4 shows the mechanism of magnetic resonance (MR) method. The Single loop has 25 cm in radius that is a role as driving circuit supplied by a sine

wave with frequency 9.9 MHz. This single loop couples inductively to the source coil and transfer entire wireless power. The load coil has a light bulb. This light bulb is turned on when wireless power arrives at the load coil through device coil. The source and device coil are aligned coaxially. The parameter ' K ' presents a coupling coefficient between the source coil and device coil. When the distance increase between the source coil and the device coil, the coupling coefficient decrease exponentially in Fig 1.3.4. This means that the coupling coefficient is related to how many the source coil transfer magnetic fluxes to the device coil. They successfully powered a 60 W light bulb wirelessly over a distance 2.4 m with 40% efficiency between the magnetic coils. Owing to this characteristic of MR systems, it is possible to transfer power over greater distances than MI systems. The efficiency of MR systems is higher than MI systems because the magnetic fluxes that are not guided to the Rx coil disappear and, return to the Tx coil. Also, this technique is harmless to the human body because MR systems use magnetic waves rather than electromagnetic waves propagated by RF systems which can be absorbed by the human body.

1.4 Theory of magnetic field

To get the high efficiency of power transmission using magnetic wave, it needs to generate strong magnetic field. Magnetic field is formed by a number of magnetic lines of force. In the case of the solenoid type that is one of general structures to make the magnetic field, the magnetic field is formed in the center of the solenoid. A part of the solenoid wire generates the magnetic lines of force like loop when the wire is supplied by time varying current. Due to the solenoid structure, the magnetic lines generated by conducting wires are gathered in the center of the solenoid in Fig 1. 4. This mechanism is presented as the follow: [13]

$$\int Bdl = Bl = \mu_o in$$

$$B = \mu_o i \frac{n}{l} \quad (1)[13]$$

Where ' μ_o ' is the magnetic constant, ' i ' is the current, ' n ' is the number of turns, ' l ' is the length of solenoid, and ' B ' is the magnetic flux density. This model is valid in the air. With having strong magnetic field, it needs to increase with the number of turns per unit length and time varying current. To get both the number of turns per unit and time varying current, the solenoid coil is formed as a big coil because the time varying current is related to the resistance that the thick conducting wire's resistance is low. Also, the number of turns can be wound as possible in the big area.

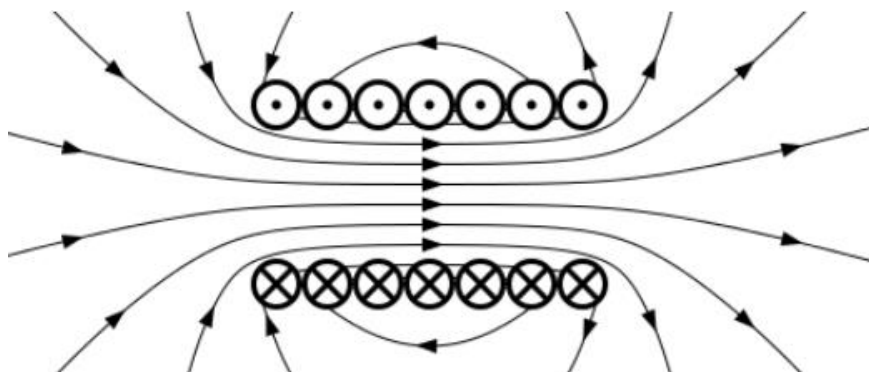


Fig 1.4.1 The cross sectional view of magnetic field created by a solenoid [13]

1.5 Antenna structure for power transmission

1.5.1 Coil design

Antenna models for power transmission have been studied to optimize a magnetic design. In order to activate magnetic waves, the coil design must be optimized. Because of this reason, the coil shapes have been studied to maximize magnetic fields [5].

Antenna designs include several shapes such as circular, square, rectangular and particular shapes including a splitting of the available area into electrically parallel connected segments and a double layer with a same coil shape at each layer in Fig 1.5.1.

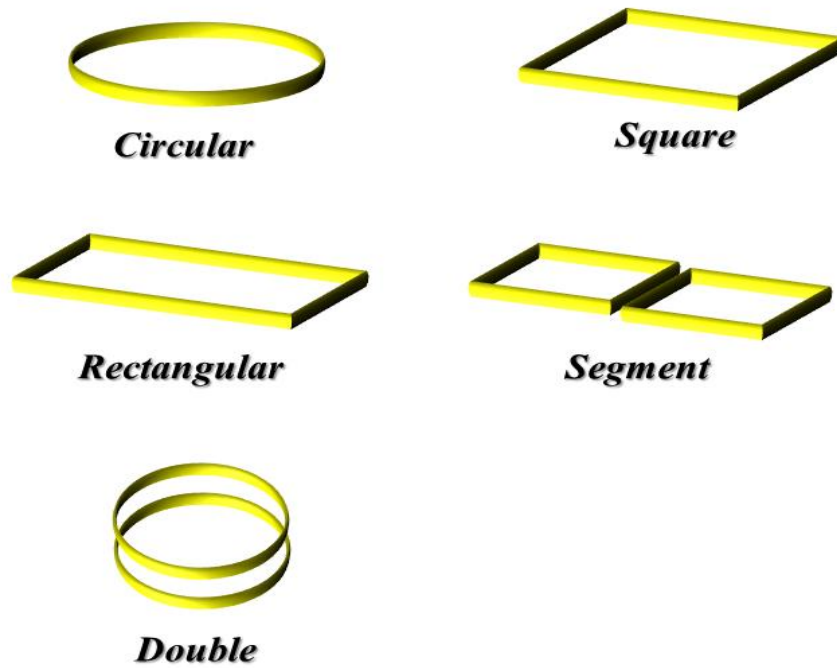


Fig 1.5.1 Various types of a coil

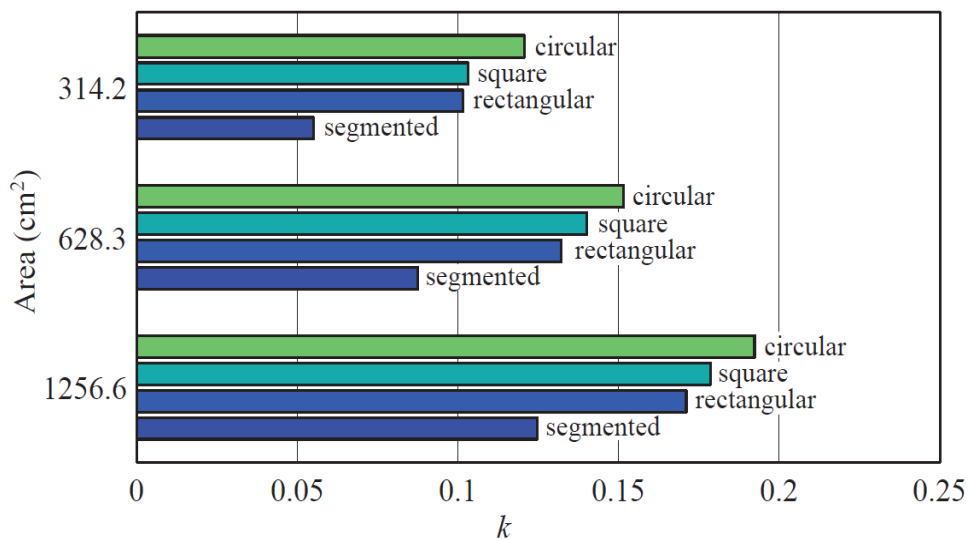


Fig 1.5.2 Comparison of the results of the 3D FE simulations for magnetic coupling k [5]

When comparing single layers over double layers, a given same size, square and rectangular shapes show approximately the same magnetic coupling ' k '. Circular shapes have higher magnetic coupling ' k ' than square and rectangular shapes with the same area in Fig 1.5.2 [5]. The circular model curved lines at the edge. The curved lines reduce the conflict of flowing time varying current. On the contrary, square and rectangular shapes have right angles at each corner. This means that coils with angular parts make it difficult to flow time varying current well. Due to this reason, the magnetic field is weaker than circular shapes. In the case of particular shapes with segmented coils, the parallel connected model is insufficient to maximize the strong magnetic flux rather than another layer model. However, the double layer is different. A double layer coil better optimizes the magnetic field compared with a layer coil of the same diameter [1]. The outer diameter is 5 mm, the inner diameter is 1.25 mm, and the coil thickness is 10 μm . The width and spacing have 15 μm and 20 μm . Though the diameters of both are the same, the number of winding is approximately double in Table I [1]. The inductance value of the double layer has 45 μH , this value is higher than the single layer (12 μH) about 4 times. Also, a self-resonance frequency point of the double (6.5 MHz) is lower than the single layer's self-resonance frequency point (127 MHz) due to the value of inductance. In the case of a quality factor (Q) at 2.64 MHz, the double layer has 5.9 compared with the single layer with 3. Q-factor is to describe a characteristic of resonator's bandwidth relative to its center frequency. High Q-factor indicates a lower rate of energy loss relative to the stored energy of the resonator. So, the double layer's energy loss is lower than the single layer. Due to these reasons of an inductance value and Q-factor, the voltage gain of the double layer is higher than the single layer about 3.5 times. Therefore, with an increase in the layer of the coil, more and stronger magnetic fields are formed.

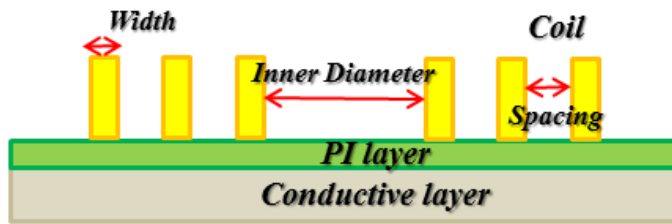
TABLE I. Comparison of Single and Double layers [1]

	Single layer	Double layer
Inductance (uH)	12	45
Q-factor at 2.64 MHz	3.0	5.9
Self- resonance (MHz)	127	6.5
Voltage gain	0.051	0.18

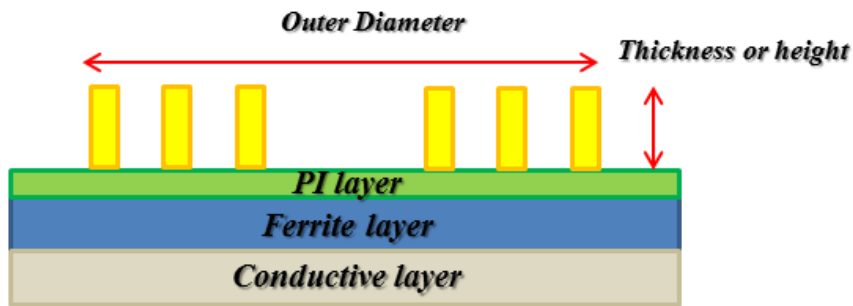
1.5.2 Magnetic Core (MC) structure.

Larger coil structures can generate magnetic field more easily than smaller ones. The efficiency of a coil structure decreases steeply as its diameter decreases because of a narrow magnetic field. In the case of micro-scales, the working area from the magnetic field is incredibly small. This small working area is a hot issue in micro-size research. Some research groups have attempted to improve the size effect. As mentioned in the coil design, the double layer is one of the alternatives [1][14][15], but this idea is not suitable for the micro-size coil structures due to a complex fabrication process and spacing limitations. Instead of this design idea, a ferrite layer has been used in small-sized coil structures [1][16][17]. The ferrite layer is located under the coil structure. The ferrite layer reflects magnetic fluxes in downward direction. The effect of the ferrite layer was simulated [1]. When the ferrite with a relative permeability ($\mu_r = 200$) is used under the flat spiral coil, the inductance increase is 80 % at the distance of 10 um, and 64% at the distance of 100 um compared with no ferrite. Also, the ferrite with a high relative permeability ($\mu_r = 500$) has higher inductance values compared with the ferrite with a relative per-

meability ($\mu_r = 200$) over whole ranges of distance between a coil layer and a ferrite substrate. Figure 1.5.3 indicates the design of a coil with the ferrite layer and without the ferrite layer. The ferrite layer is located on the conductive layer for example Si (silicon) layer. This is a basic structure of fabricating a single coil with ferrite layer to increase with inductance values.



(a)



(b)

Fig 1.5.3 Parameters of a single layer on the ferrite layer and no ferrite layer. (a) Single layer without the ferrite layer. (b) Single layer with the ferrite layer [1]

In this study, we created a magnetic core (MC) structure in the center of the coil structure. Normally, MC structure has been used in a transformer to send an electrical energy from the primary coil to the secondary coil [18][19]. The electrical energy from the primary coil is transformed into magnetic fluxes. These magnetic energies flow

to the MC structure. Eventually, the magnetic fluxes are changed into electrical energy in the secondary coil. Our MC structure is based on this characteristic of transformer's magnetic core. If a material is under a magnetic field, the magnetic property of this material is changed. This process is called magnetization. The magnetic flux density caused by a coil structure is related to a channel of a relative magnetic permeability (μ_r) in Fig 1.5.4. An MC with a high relative magnetic permeability (μ_r) is easy to guide magnetic field strongly. For example, nickel (Ni) has a relative magnetic permeability of about '80' which means that an MC consisting of nickel (Ni) has strong magnetic flux density, especially compared to air, which has a relative magnetic permeability of about '1' [20]. Therefore, the higher time varying current to the coil, the more that the magnetic flux density will increase by using an MC with high relative magnetic permeability.

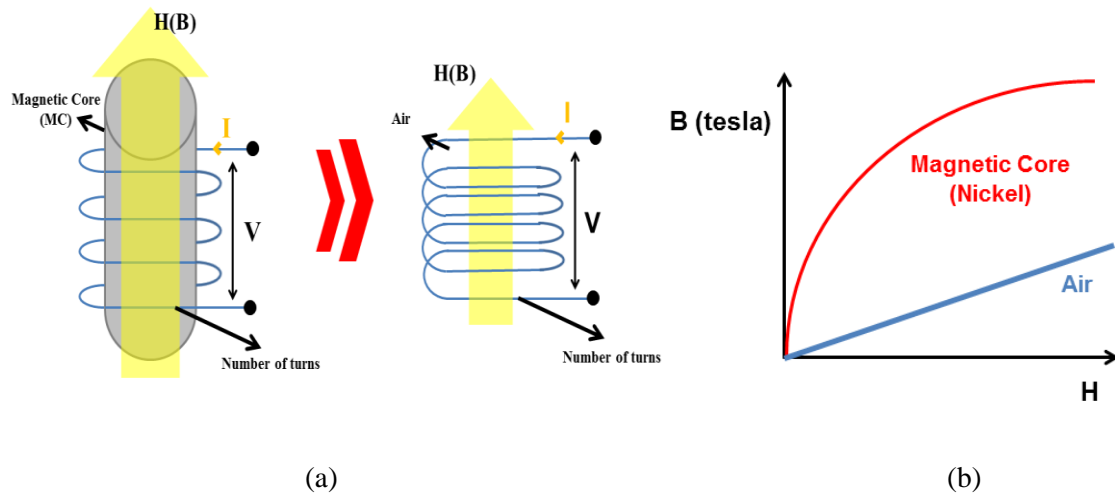


Fig 1.5.4 The influence of magnetic core (MC) in the coil. (a) The difference of a magnetic field strength (H) when using a magnetic core (MC) and air. (b) Magnetic flux density (B) curve: Nickel (Ni) and Air [20]

II. EXPERIMENT DETAILS

2.1 Fabrication of the basic coil

To validate the electrical characteristics of MI and MR systems, a basic flat spiral structures with an outer diameter of about several millimeter and various winding turns is needed. Most micro-size coil structures were fabricated on Si-SiO₂ substrate. But this Si-SiO₂ substrate has a limitation that makes the parasitic capacitance between coil and Si layer. The parasitic capacitances reduce the electrical characteristic of an inductance value of the flat spiral coils. In the case of a thin SiO₂ layer, it makes higher capacitance than a thicker SiO₂ layer. We used a glass substrate to reduce the parasitic capacitances.

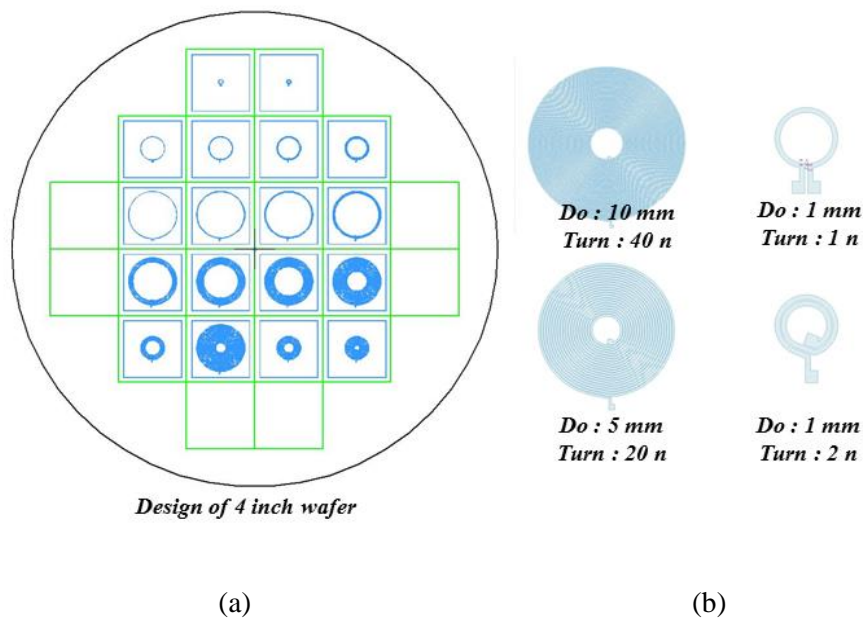


Fig 2.1.1 The design of 4 inch wafer for various coils. (a) The location of each coils: 10 mm, 5 mm, and 1 mm. (b) The coils with various outer diameter (10 mm, 5 mm, and 1mm) and turns (40 n , 20 n, 2 n, 1n)

Before the fabrication process, the conditions with various diameters and turns were designed by using the My CAD program on a photolithography mask in Fig 2.1.1. The turns are changed from 1 n to 40 n until the turns are maximized. The outer diameter also changed from 1 mm to 10 mm. There are 3 kinds of the outer diameter: 10 mm, 5 mm, and 1mm. The design of a coil with the outer diameter (10 mm) has 9 kinds of turns: 1 n, 2 n, 3 n, 5 n, 10 n, 15 n, 20 n, 30 n, and 40 n. Another design of a coil with the outer diameter (5 mm) has 7 kinds of turns: 1n, 2 n, 3 n, 5 n, 10 n, 15 n, and 20 n. The last design of a coil with (1 mm) has 2 kinds of turns: 1 n and 2 n. This coil designed is a source of a photo mask for a photolithography. The photo mask was made by a sodalime and chrome. The parameter of the photo mask is that are size (126.6 mm x 126.6 mm), thickness (2.3 t), and specification ($10 < \mp 0.5 \mu\text{m}$).

The photoresist (ZXR-601) was coated on a glass substrate to a thickness of about 2 μm . The revolution per minute (rpm) is about 1000. The lower rpm makes thicker thickness. To be solid state, the coated substrate was baked on a hot plated about 100 °C for 2 minutes. Next step was to exposure ultraviolet ray (UV) using the photo-make for 2.5 second. This step is important because it needs to consider a thickness of a photoresist. A short exposure time cannot bind a chain of a photoresist in the deep place. After ultraviolet ray (UV) photolithography, the coil layer with the Ti (50 nm) / Au (500 nm) was formed by using a sputtering technique. The Ti (50 nm) layer enhances the adhesion between the glass and the Au layer. After sputtering the Ti / Au layer, unwanted photoresist parts were removed by using a lift-off technique in Fig 2.1.2. The outer diameter (D_o)s of the coil structures were changed from 10 mm to 500 μm . Their parameters were fixed at a thickness of ($t = 500 \text{ nm}$), a width of ($w = 80 \mu\text{m}$). The spacing between turns was ($s = 20 \mu\text{m}$).

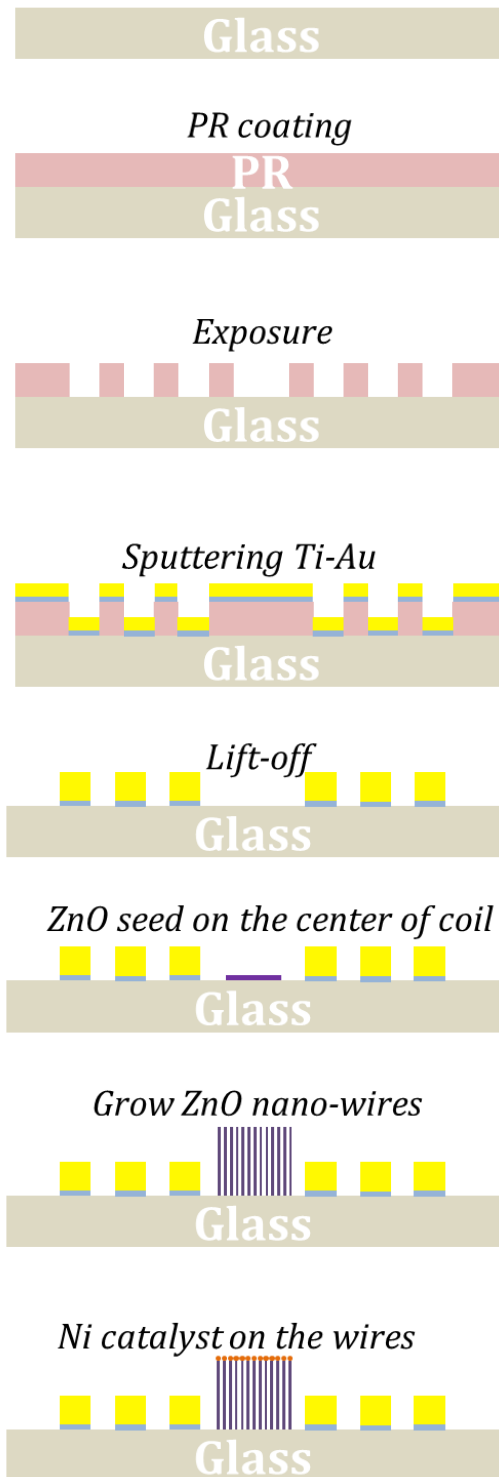
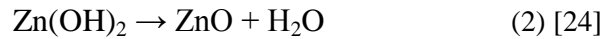
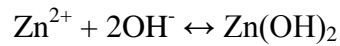
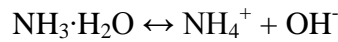
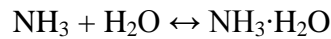
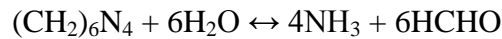


Fig 2.1.2 The Process of photolithography and growing ZnO nano wires – Ni layer

2.2 Designing a magnetic core (MC) structure

The magnetic core (MC) structure consisted of ZnO nano wires and a Ni layer. The ZnO nano wires served as frame to coat the Ni layer. The 50 nm ZnO seed layer was deposited by using the sputtering system and a photolithography process on the center of a basic flat spiral coil pattern in Fig 2.1.2. After the lift-off process of the ZnO seed layer, we used the hydrothermal process which is possible to grow uniformly ZnO nano wires on the substrate [21][22][23]. The sample was suspended upside down direction using plastic tools and was then dipped in a glass bottle filled with 20 mM solution which was mixed by hexamethylenetetramine and zinc nitrate hexahydrate.



The nutrient solution was composed of a 1:1 ration of zinc nitrate hexahydrate and hexamethylenetetramine (HMTA). Zinc nitrate salt provides Zn²⁺ ions required for building up ZnO nanowires. Water molecules in the solution provide O²⁻ ions. The glass bottle was heated in a vacuum oven at 70°C for 48 hours in Fig 2.1.3. The grown ZnO nano wires were rinsed with an IPA solution to clean the surface of the sample. Then the Ni layer was coated on the vertical ZnO wires by photolithography, the sputtering and the lift-off process in Fig 2.2.1.

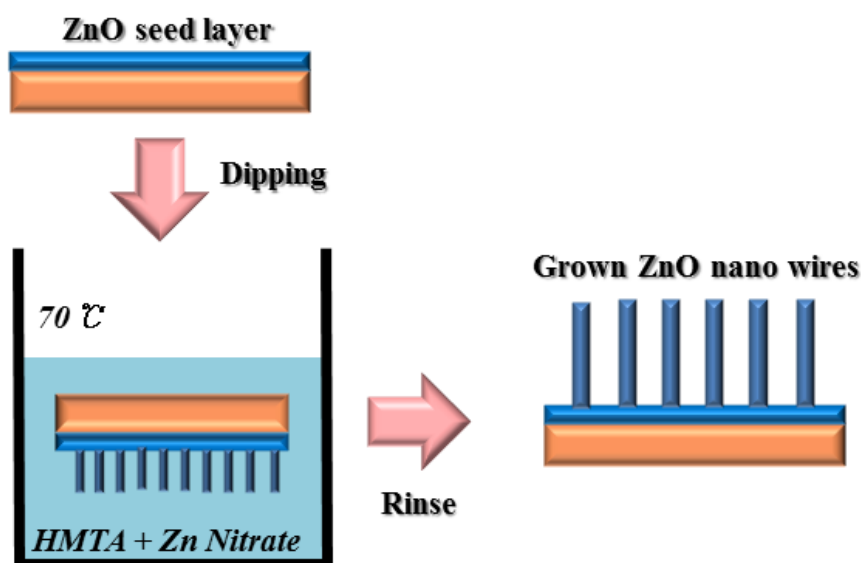


Fig 2.2.1 The Process of growing ZnO nano wires

2.3 Experiment Condition

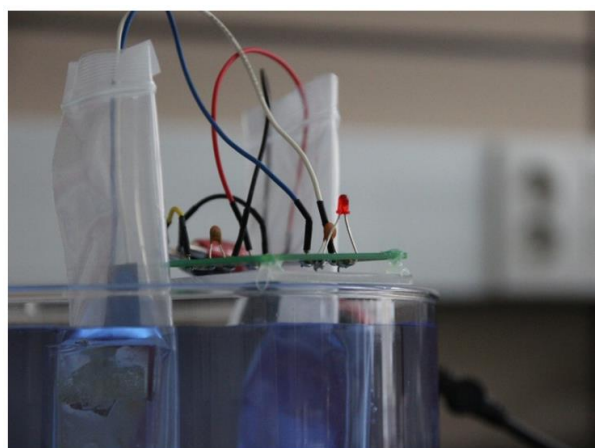
The inductance, the series resistance, and the self-resonant frequency of various antenna structures were measured by using an impedance analyzer and a network analyzer (Agilent technology E5061B). The frequency range was found to be from 100 kHz to 30 MHz. The inner connection pad was connected to a test fixture (Agilent technology 16047E) by using a wire bonding technique where the thickness of the aluminum wire was about 1 mil (25 μm) in Fig 2.3.1 (a). To measure the power transmission efficiency in the air and the water, the antenna structures were divided into two main parts in Fig 2.3.1 (b)(c). One was the Tx designed by the flat spiral coil with the inductance value about $L \approx 12.33 \mu\text{H}$ in the macro scale. The other was the Rx that was also designed by the flat spiral coil with the MC and without the MC structure.



(a)



(b)



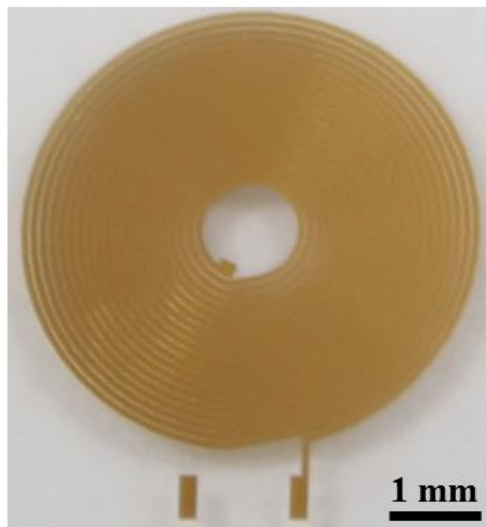
(c)

Fig 2.3.1 The experiment condition (a): Wire bonding between the inner pad and outer connection pad (b) Power transmission setting in the air (c) Power transmission setting in the water

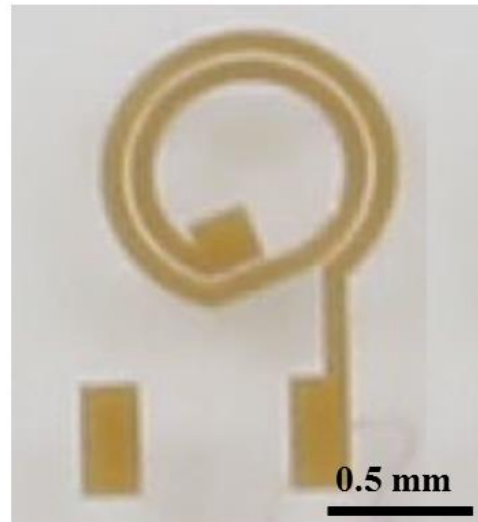
III. RESULTS AND DISCUSSION

3.1 Results of micro size antennas for the magnetic induction

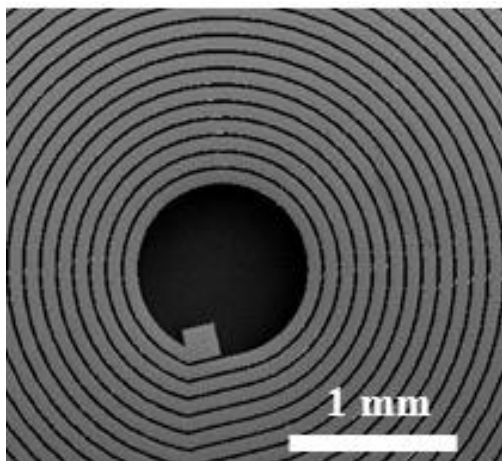
After using the process of the photolithography and lift-off, the images of micro size antennas were taken in Fig 3.1.1. Figure 3.1.1 (a), (b) shows the optical micro images with same width (80 μm), thickness (500 nm) and spacing (20 μm). The inside of pad is connected to the left bottom of the pad by using a wire bonding. The diameter of a wire bonding is about 25 μm , so the pad is designed to be bigger than a size of width. Figure 3.1.1 (c), (d) indicate the scanning electron microscope (SEM) images for 10 mm 20 n (outer diameter = 10 mm and turn = 20 n) and 1 mm 1 n. Figure 3.1.2 (a), (b) present the spacing between widths and the thickness. The length of spacing is fixed on 20 μm . The thickness is checked to use a micro ruler. The goal of thickness is 500 nm to use the sputtering system, so the thickness of Au is quite exact. Figure 3.1.2 (c) shows the thickness of a coil. The thickness was measured by using a surface profiler, the red area indicates a bottom of a coil and the green indicates a sputtered area of the coil. The difference of the green and the red is the thickness of the coil about 5124 \AA (512 nm). The edge of both sides of the green area has sharp needles that is higher than a flat green area. This reason comes from the process of the photolithography and the lift-off. This unwanted edge effect can be seen in Fig 3.1.2 (a). The thick lines of the edge on the width can make an impedance to be higher due to imperfect shapes. To overcome this problem, it needs to fabricate another process such as an electro plating skill. However, the photolithography and the life-off process are easier and not to waste time of designing coil patterns. So, in this study, we used the process of the photolithography and the life-off.



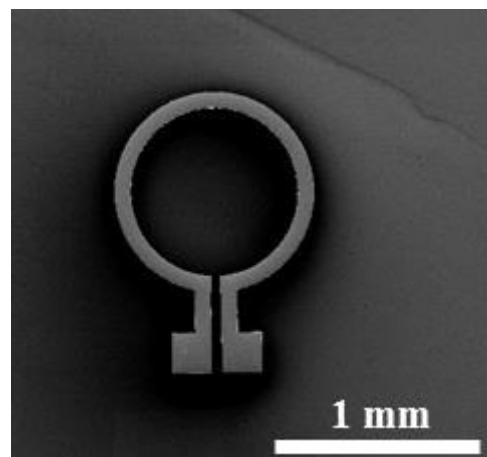
(a)



(b)

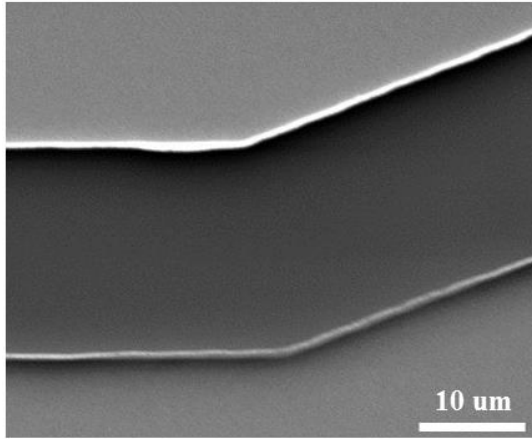


(c)

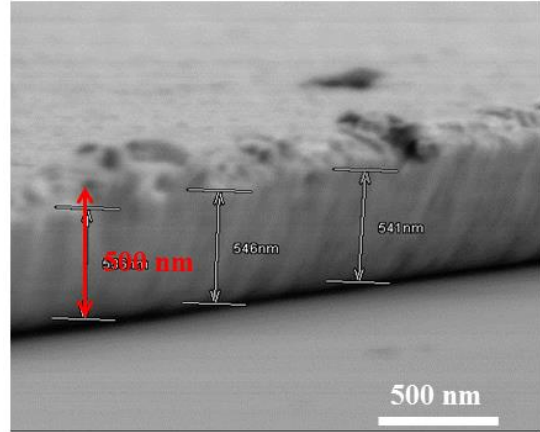


(d)

Fig 3.1.1 Optical images and scanning electron microscope (SEM) images (a) Optical image for 5 mm 20 n (outer diameter = 5 mm and turn = 20 n). (b) Optical image for 1 mm 2 n (outer diameter = 1 mm and turn = 2 n). (c) The center of SEM image for 10 mm 20 n (outer diameter = 10 mm and turn = 25 n). (d) SEM image for 1 mm 1 n (outer diameter = 1 mm and turn = 1 n)



(a)



(b)



(c)

Fig 3.1.2 The SEM images of a boundary between a width and spacing (a) SEM image for the spacing between widths. (b) SEM image for thickness of a coil (c) The thickness of a coil by measuring a surface profiler

3.2 Electrical characteristic of basic coils

3.2.1 Theoretical values of an inductance

Before measuring the electrical characteristic of basic coils, the theoretical inductance and DC resistance values were calculated by using the expressions for a basic single layer spiral inductor and a basic electrical DC resistance [25].

$$R = \sigma \cdot \frac{l}{S} \quad (3) [25]$$

One expression of basic DC resistance needs three parameters: the length of the spiral coil ($l - m$), the spiral coil cross section ($S - m^2$) and the electrical resistance of the spiral coil (σ - ohm. m). We used Au material to fabricate the spiral coil shape. Au has an electrical resistance about $2.4 \cdot 10^{-8}$ [ohm. m] and the length of a spiral coil depended on the outer diameter length. The cross sectional area is same to $4.0 \cdot 10^{-11}$ [m^2]. The electrical DC resistances are calculated from 1mm 1turn (outer diameter = 1mm and winding = 1n) to 10mm 40 turns (outer diameter = 10mm and winding = 40) in and are shown in Table II. The length of the spiral coil is related to DC the resistance. Increasing with the length of the spiral coil where the value of cross section and the electrical resistance are same, the DC resistance increases. In the case of 10 mm 40turns, the DC resistance (451.0Ω) is higher than other cases because the resistance is proportional to the length of the spiral coil. On the contrary, the 1 mm 1turn has the lowest DC resistance (1.2Ω) among whole models of a spiral coil. The other expression of an inductance value is described as follows: [14][25][26]

$$L = \frac{\mu \cdot n^2 \cdot d_{avg} \cdot C_1}{2} \left(\ln\left(\frac{C_2}{\rho}\right) + C_3 \cdot \rho + C_4 \cdot \rho^2 \right) \quad (4) [25]$$

TABLE II. DC resistance of the theoretical and I-V characterization system

Type	Parameters		
	Outer Diameter (mm)	Turn (n)	Resistance (Ω)
Theoretical	1 mm	1	1.200
	5 mm	10	75.00
		20	112.8
	10 mm	20	302.2
		40	451.0
	I-V Characterization system	1 mm	1
5 mm		10	155.5
		20	277.7
10 mm		20	378.7
		40	849.4

The parameters are a material permeability (μ), a number of turns (n), an average diameter (d_{avg}), coefficients ($C_1 \sim C_4$) and coil fill ratio (ρ). The coefficients ($C_1 \sim C_4$) are related to the shape of the flat spiral coil. We chose circle parameters as ‘1.00’, ‘2.46’, ‘1.00’ and ‘0.20’ for C_1 to C_4 respectively. The material permeability (μ) of Au is about $1.256 \cdot 10^{-12}$ [H/m]. The coil fill ratio (ρ) and average diameter (d_{avg}) depend on the outer diameter and the inner diameter. The calculated results are shown in Table III. With increasing diameter and turn, the inductance value increases slightly. In the case of 10 mm 40 turns (outer diameter = 10 mm and turn = 40 n), the inductance value is about 8.407 uH. This value is higher than another inductance value. When the parameters (coefficients, a material permeability, thickness, width, and spacing) are fixed, the inductance value is dependent on the turns and an outer diameter. From these results, the turn and the diameter of a flat spiral coil are important factors to enhance the inductance value.

TABLE III. The theoretical and measured inductance values

Type	Parameters		
	Outer Diameter (mm)	Turn (n)	Inductance (H)
Theoretical	1 mm	1	1.752n
	5 mm	10	0.577u
		20	1.059u
	10 mm	20	4.619u
		40	8.407u
	Measured	1 mm	1
5 mm		10	1.025u
		20	1.761u
10 mm		20	5.505u
		40	9.764u

3.2.2 Measurement values of resistances and inductances

The electrical DC resistance values of flat spiral coils employing Au thin film of about 500 nm structure were measured by using a Probe station and I-V characterization (KEITHLEY 4200-SCS semiconductor characterization system). The voltages were swept from -5V to +5V with a step voltage of 0.01V. Table II shows the measured electrical DC resistances. As can be seen from results, 10 mm 40 turns (outer diameter = 10 mm and turns = 40 n) has a higher series resistance than the other coils at about 849.4 ohm. On the contrary, the resistance of 1 mm 1 turn of about 6.241 ohm is the lowest resistance value among the other coils. 10 mm 10 turns has approximately 141 times of the resistance. This is due to an outer diameter and turns. The more the turns and outer diame-

ter increase, the more electrical DC resistance increases. Comparing theoretical DC resistance values with measured DC resistance values, there are some differences. In the case of 1mm 1turn (outer diameter = 1 mm and turn = 1n), the difference of DC resistance is 5.041Ω between the theoretical value and the measured value. With increasing the outer diameter (1 mm to 10 mm) and the turn (1n to 40 n), the difference of DC resistance increases with 398.4Ω . The reason is that the theoretical value was calculated by using a perfect electrical resistance (Au). However, the electrical resistance of fabricated coils was different. The real measurement of a sheet resistance is about $0.17196 [\text{ohm} / \text{Cm}^2]$, so the real electrical is $8.598 \cdot 10^{-8} [\text{ohm} \cdot \text{m}]$. This real electrical resistance is higher than the theoretical electrical resistance value ($2.4 \cdot 10^{-8} [\text{ohm} \cdot \text{m}]$) about 3.58 times. It came from the process conditions which the fabricated coil was deposited by the sputtering system. This sputtering system does not form the perfect Au structure due to its mechanical process. It makes the bulk type of Au structure with different electrical resistance of Au. Therefore, the theoretical resistances and the real resistances have deviations of the DC resistance.

The inductance values of flat spiral coils employing the Au thin film structure were measured by using an impedance analyzer from 100 kHz to 30 MHz for the size effects. Table III shows the measured inductance values for various antenna diameters, with a width of (80 μm), a thickness of (500 nm) and the turn (1 ~40 n). The inductance values dropped sharply from 9.764 μH to 11.51nH depending on the outer diameter.

Figure 3.2.1 shows the inductance values with various diameters (1 mm ~ 10 mm) and turns (1 n ~ 40 n). In the case of 1 mm (outer diameter) the inductance values are lower than any other cases. With the same turn (1 n), the 10 mm (outer diameter) is a high inductance value about 140 μH and other cases with same turn (10 n and 20 n) show same results. Therefore, the inductance values are dependent on turns and a size of an out-

er diameter. Comparing theoretical inductance values with measured inductance values, the difference of the inductance is smaller in the case of 10 mm (outer diameter = 10 mm). With decreasing the outer diameter, the difference between theoretical and measured inductance increases. One of reasons is the wire bonding. To measure the inductance value, a coil needs to connect the impedance analyzer kit. A length of a wire bonding makes the inductance to increase in the case of a small size of coils. The other reason is the Au material permeability. The theoretical Au material permeability is the perfect condition. However, the measure Au material permeability is different compared with the theoretical value due to the bulk structure. These two reasons make the gab of inductance values.

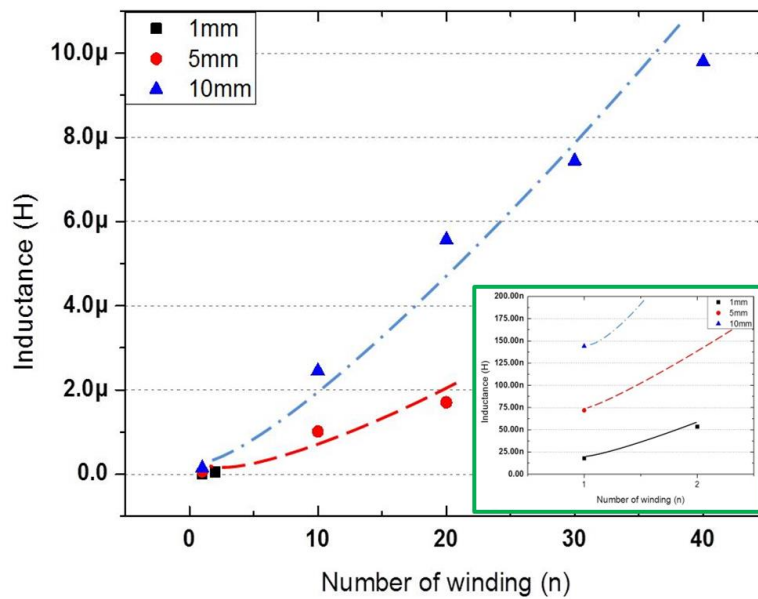
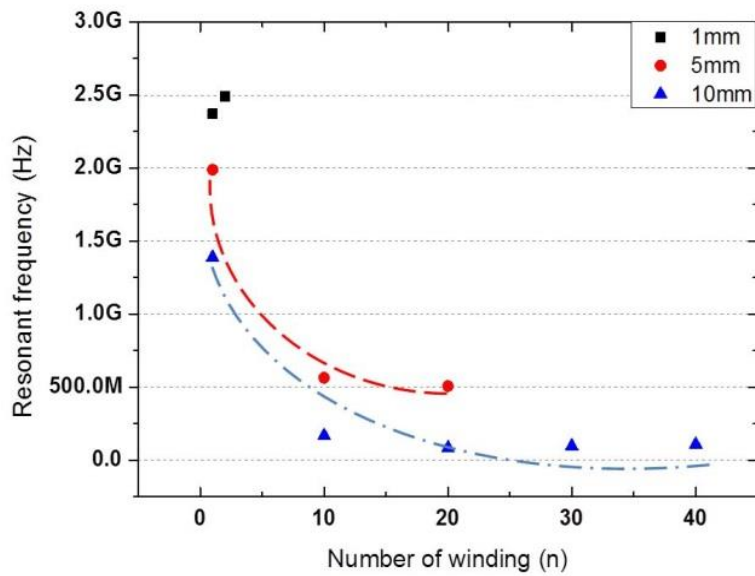


Fig 3.2.1 The inductance values of coils with various diameters (1 mm ~ 10 mm) and turns (1 n ~ 40 n)

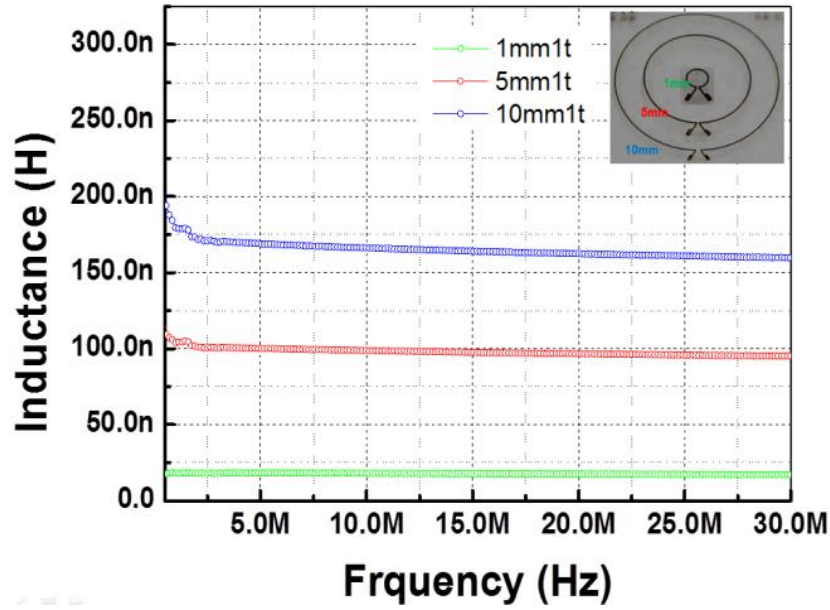
3.2.3 Measurement values of a self-resonant frequency

These inductances are related to a self-resonant frequency [27][28]. To check the self-resonant frequency, we performed an experiment to measure self-resonant frequencies according to different inductances in Fig 3.2.2. The frequency range was

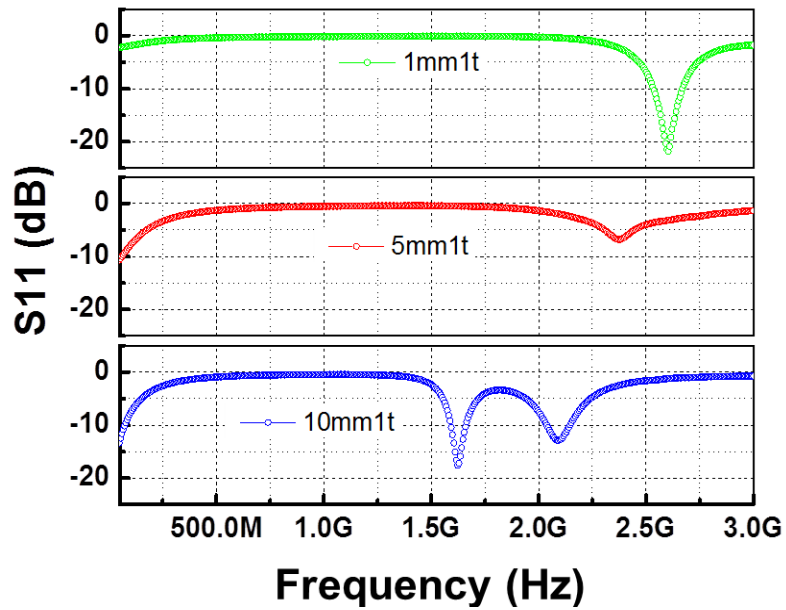
swept from 300 kHz to 3 GHz. Figure 3.2.2 (a) shows the each self-resonant frequency over increasing with outer diameters (1 mm ~ 10 mm) and turns (1 n ~ 40 n). In the case of 10 mm (outer diameter), the self-resonant frequency values with 40 turns is lower than another turn. Also, in the case of a same turns (20 n), self-resonant frequency value with 10 mm (outer diameter) is lower than 5 mm (outer diameter) case. To be specifically, the self-resonance frequency of the coils is changed from 2.6 GHz to 1.6 GHz with increasing the coil diameter in Fig. 3.2.2 (c). The frequencies correspond to 11.53 cm and 18.73 cm of the wavelength respectively in a near field. It means if the coils are used as magnetic inductance antennas, the 10 mm coil can receive or give a better power transmission for a longer distance with a high inductance than the 1 mm coil, since the magnetic inductance generally shows high efficiency of the transmission under the near field size.



(a)



(b)



(c)

Fig 3.2.2 The electrical characteristics of basic flat spiral antennas (b) Inductance values of basic flat spiral antennas with various outer diameters (1 mm = green, 5 mm = red and 10 mm = blue) and the same turn (1 n) over sweeping the frequency from 100 kHz to 30 MHz. (c) S11 parameters (dB) of basic spiral antennas over sweeping the frequency from 300 kHz to 3 GHz

3.3 Electrical characteristics of magnetic core (MC) coil

A flat spiral coil with a small outer diameter and turn has a low inductance and high resonance frequency due to the limitation of the size effect. To overcome this size effect, the core structure formed by a ferro-magnetic material is suggested in the center of a coil pattern. Normally, if the ferro-magnetic material is located under the coil pattern, the inductance value can be enhanced by inducing a higher magnetic flux in the center [15]. The magnetic flux density (B-field) is dependent on the core material permeability which is related to the quantity of the magnetic moment.

$$B = \mu_r \mu_0 H [\text{weber} / \text{m}^2] \text{ Or } [T (\text{teslar})] \quad (5) [20]$$

Where, μ_r is the core material magnetic relative permeability, μ_0 is the magnetic constant, and H is the magnetic field. In this study, a micrometer size of the MC is formed inside the spiral coil structure to enhance the magnetic field (Fig 3.3.1 (a), (b)). The MC made by the ferro-magnetic material can help to focus the magnetic field in the center of the flat spiral coil and to reduce the loss of magnetic fields escaping from the center. To enhance the focusing effect with directionality, a vertical three dimensional (3D) structure can be added. If we choose nano wires as the 3D structure, the increasing effective area is also expected, so that the enhancement can be maximized. Here, ZnO nano wires are used for the 3D core structure, since ZnO nano wires can be grown below 100°C with good structural properties. The low process temperature does not damage the coil structure or the glass substrate. By controlling the preferred orientation of the seed layer for ZnO nanowires, the ZnO nano wires are grown vertically as shown in Fig 3.3.1 (c). The measurement of X-ray diffraction (XRD) and photo-luminescence (PL) spectrum

are the preferred orientation of nano wires [29][30]. Figure 3.3.2 (a), (b) show that nano wire is formed as a single crystal. An SEM image of the MC structure with ZnO nano wires coated by the Ni layer is shown in Fig 3.3.1 (d).

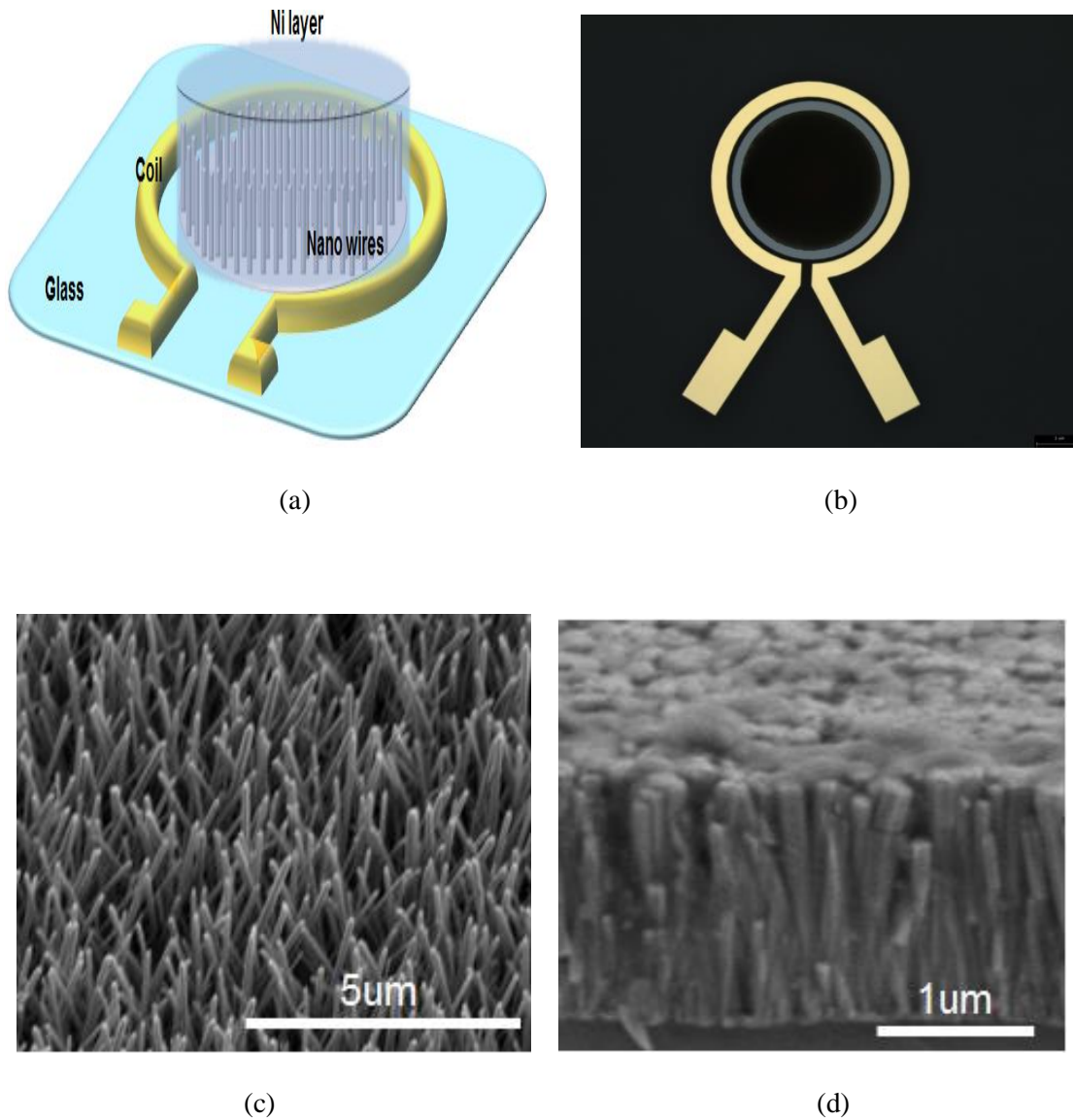
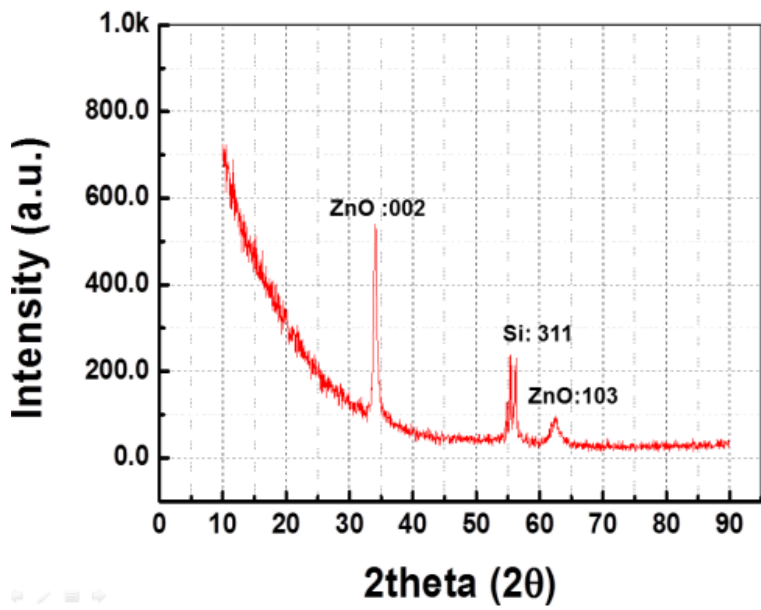
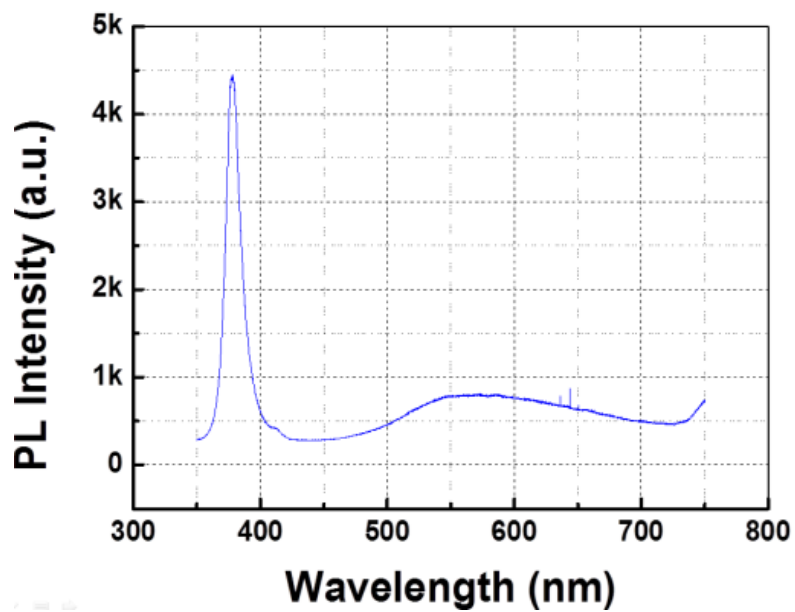


Fig 3.3.1 The flat spiral antenna structure with the magnetic core (MC) consisting of ZnO nano wires and the Ni layer (a) The 3D schematic diagram of the suggested structure. (b) Optical microscope image of the structure (c) Scanning electron microscope (SEM) image of ZnO nano wires grown by a hydrothermal method (d) The cross section SEM image of ZnO nano wires after sputtering the Ni thin film

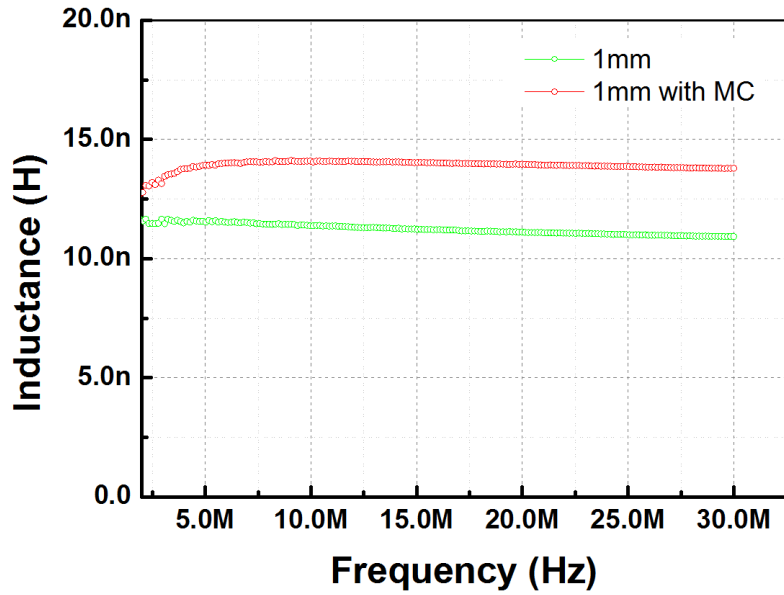


(a)

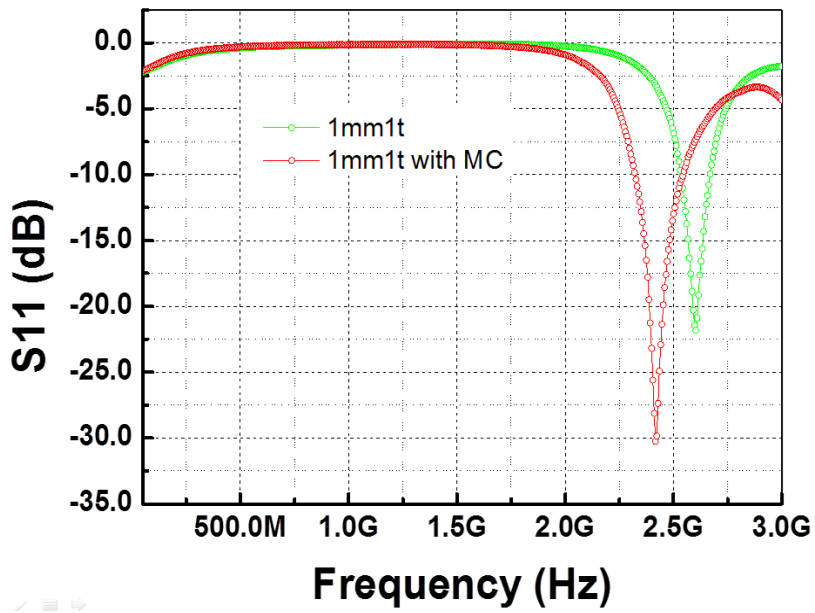


(b)

Fig 3.3.2 The data of ZnO nano wires in XRD and PL (a) XRD peaks of ZnO nano wires on glass substrate (b) PL analysis of ZnO nano wires on the glass substrate



(a)



(b)

Fig 3.3.3 Electrical characteristics of 1 mm 1 turn antenna structure with the MC and without the MC (a) Inductance values of 1 mm 1 turn with the MC (red) and without the MC (green) : 13.9 nH with the MC and 11.5 nH without the MC at 1 MHz (b) The S11 parameters with the MC and without the MC. The self-resonant frequency point decreases from 2.6 to 2.4 GHz when the 1mm antenna has the MC

Figure 3.3.3 shows the electro-magnetic characteristics of the MI antenna with the MC structure. Even though the MI antenna with the MC structure is occupied with the same space ($D_o = 1 \text{ mm}$), the structure has high inductance due to the core effect. For the frequency dependence, the antenna structure with the MC can reduce the reflection power measuring S_{11} parameter (dB) from -22 dB to -30 dB by lowering the resonance frequency (Fig 3.3.3 (b)).

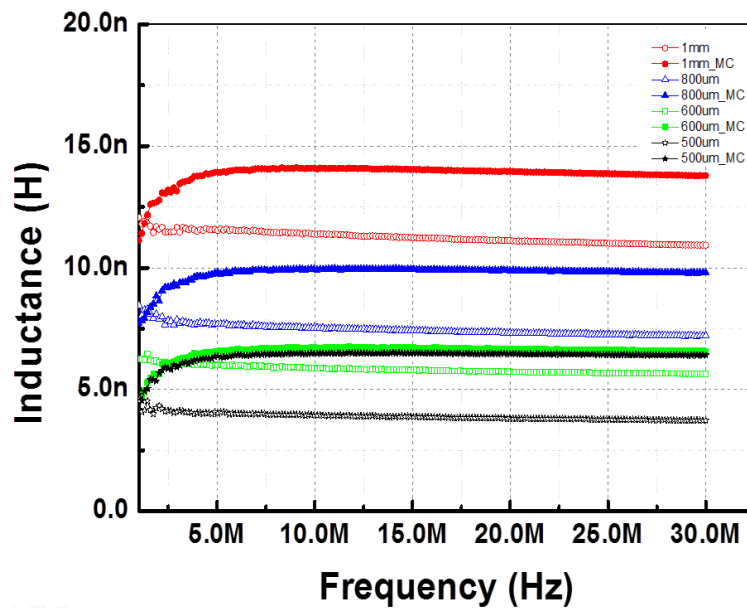


Fig 3.3.4 The inductance values under an outer diameter (1 mm) with MC and without MC

A flat spiral coil with an outer diameter (1 mm), it is insufficient to apply to a human implanted system because the flat spiral coil like a role of an antenna, it takes up much space about 70% in a human implanted device. Getting a flat spiral coil with a small size of an area is important. Figure 3.3.4 shows flat spiral coils with MC under a diameter (1 mm). The turn (1 n), width (80 μm) and thickness (500 nm) are same over whole coils. The outer diameters were changed from 500 μm to 1 mm. In the case of coils with MC, the inductance values are higher than without MC. The coil with an outer diameter of 500

um has a better inductance value (6.46 nH) than 600 um (5.85 nH) with MC at 10 MHz. Therefore, to use MC on the center of a coil is a one solution to overcome the size problem.

3.4 Power transmission

3.4.1 In the Air

The goal of designing a coil with a high inductance value is to get a high efficiency of a power transmission. To verify a power transmission using MI antenna with MC or non-MC, the experiment was processed in channels of the air and water. For the Tx antenna, the macro size coil with 12.33uH was set with the function generator (Agilent technology 33250A), and digital phosphor oscilloscope (Tektronix DPO3034) at 2 MHz. We supplied $\pm 10V$ AC bias to the Tx, and then measured voltage (peak to peak) to the difference of the Rx with changing the distances between the Tx and the Rx in Fig 3.4.1.

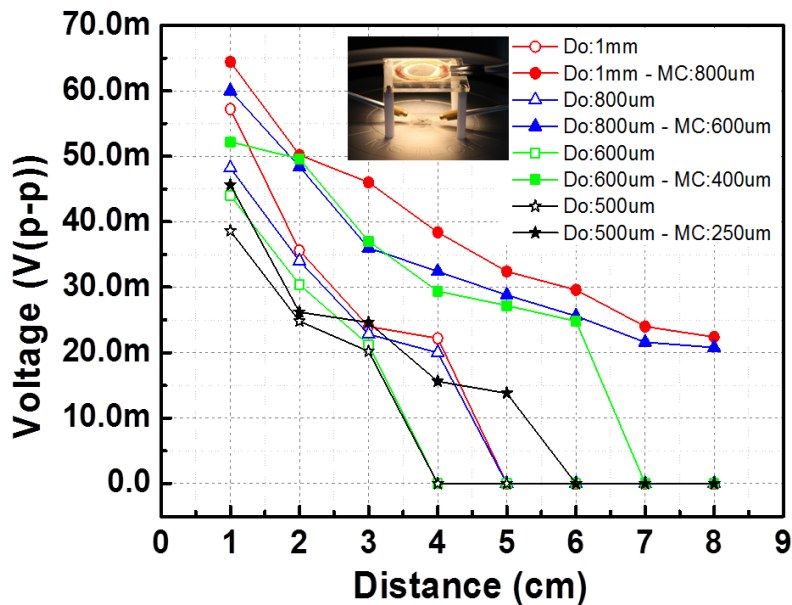


Fig 3.4.1 The power transmission in the air

In the air, the voltage of the MI antenna ($D_o = 1$ cm) with the MC (800 μ m) is higher than that without the MC at 1 cm; with MC (64 mV) and without MC (57mV). All coils with MC have high voltages compared with coils without MC over whole ranges. This difference comes from the MC effect. The MC is easy to guide the magnetic fluxes and to couple directly with the Rx coil. This interaction between the MC structure and the Rx coil makes a better effect because the induced magnetic fluxes generate the time varying current which is a source of operating electrical devices. Reducing the size of outer diameter, checked voltage values are reduced. In the comparison, the 1mm coil with MC has the high voltage (64 mV) than 500 coil without MC (38 mV) about 1.7 times.

3.4.2 In the Water

The condition of water is important in this experiment, because the human body is consisted of water about 80 % [31]. The coils were set to outer diameter ($D_o = 1$ mm) and having MC or not. In the water, the voltage of the MI antenna with the MC was measured about 63 mV at 1 cm in Fig 3.4.2. The checked voltages with MC or non-MC in the water or air are similar to each other. This result means that the MI system is not quite affected to channel conditions, it is possible to transfer power to a human body. Although the MI antenna structure with the MC shows the improvement of the efficiency of the power transmission in the air and the water, the efficiency of the medium is quite low. Some reasons which are a setting frequency, a direct measurement without an electrical matching, and a large distance compared to the antenna size can make the low efficiency result.

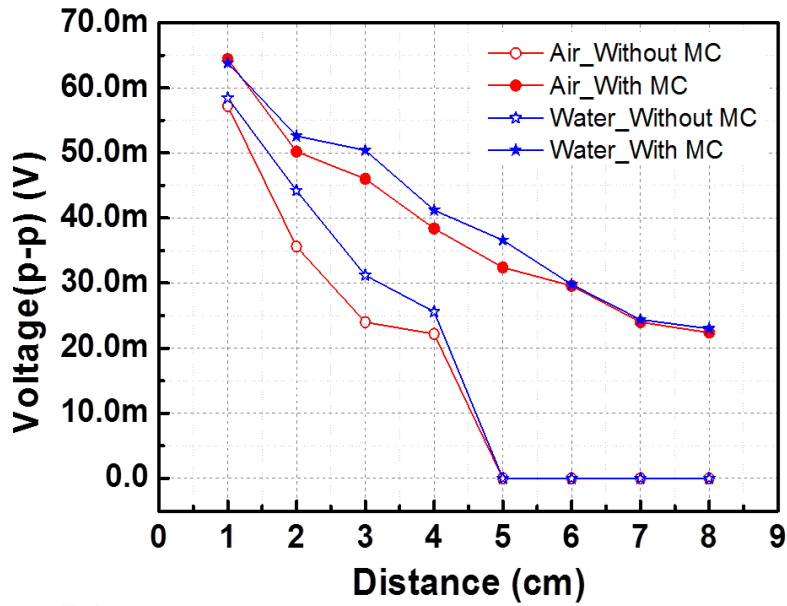


Fig 3.4.2 The power transmission in the water

3.4.3 The effect of matching a resonant frequency and impedance

With generating strong magnetic flux at Tx, Rx can easily receive the magnetic flux and converts magnetic fluxes to electric source. So, the resonant frequency and impedance matching are critical factors for the wireless transmission. Normally, the resonant frequency is related to an inductance and capacitance value [32]. Tuning the capacitance and inductance value, it can possible to set a specific frequency for power transmission. It induces the better power transmission efficiency because the power transmission system fixed by a resonant frequency point make the strong coupling between Tx and Rx without interferences of another noises. Also, the impedance matching is required to set a specific resistance value at Tx. When Function generator (Agilent 33250A) gives the magnetic antenna AC power source, it can be possible to make path loss during flowing AC current between the power source to a magnetic antenna. To reduce the path loss, the impedance is matched between power source and the magnetic antenna. In the case of a power transmission field, the 33 ohm is usually used due to good

characteristics of power transmission. In the case of a distortion, the 75 ohm is usually used. These two characteristics of a power transmission and a distortion are essential in our experiment, so we set the impedance with 50 ohm between the power source and the magnetic antenna.

Figure 3.4.3 shows the difference of efficiency power transmissions between matching resonant frequency and impedance or not. We used another Tx antenna (inductance $\approx 228 \mu\text{H}$, type = solenoid, and turn = 46 n). And we connected the capacitor (26.3 pF) and resistor (40.7 Ω) in the series model at Tx to match resonant frequency (2MHz) and impedance (50 Ω). The voltage was measured at Rx with 1mm 1turn with MC. The red line presents the matching resonant frequency with 2 MHz and impedance with 50 ohm. The green line is not matched of a resonant frequency and impedance. The voltages are only measured at the red line. On the other hand, the non-matching resonant frequency and impedance (green line) is poor at power transmission over whole distances. From this experiment, the matching resonant frequency and impedance are important in the power transmission.

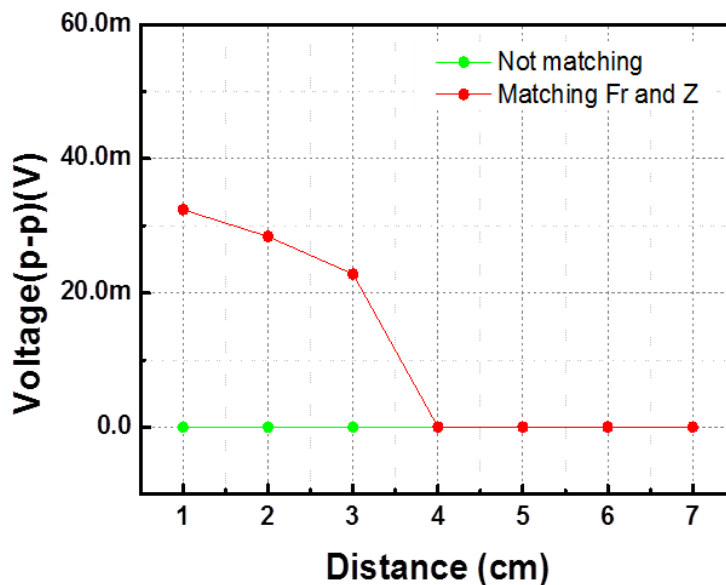


Fig 3.4.3 The matching effect of a resonant frequency and impedance

3.4.4 The effect of the power transmission over changing frequencies

In the wireless power transmission using magnetic waves, the selection of a frequency is a main issue. To find the best frequency for our study, we examined the tests over changing resonant frequencies at Tx. Figure 3.4.4 shows the measured voltages at Rx. The resonant frequencies were 1 MHz (100pF), 1.45 MHz (50pF), and 2 MHz (26.3pF) in a series model at Tx. Also, each Tx condition was matched at 50 ohm.

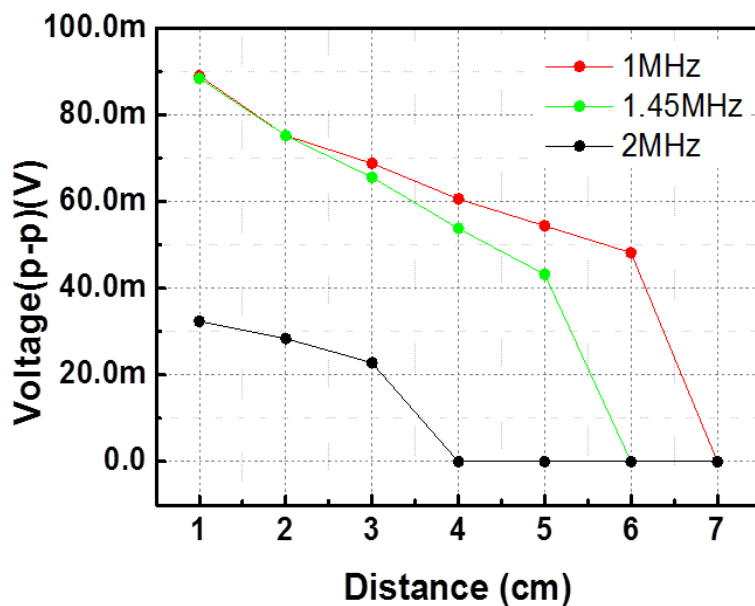


Fig 3.4.4 The effect of the power transmission over changing frequencies

The best result is checked at 1MHz (89 mV), the distance between Tx and Rx is 1 cm. The poor result is checked at 2 MHz (32 mV). With increasing with resonant frequencies, the measure voltages are reduced. From 3 cm of the distance, the voltages (resonant frequency = 2 MHz) are not checked. Over whole ranges of the distance between Tx and Rx, the red line (1MHz) presents better efficiency of power transmission compared with the green (1.45 MHz) and black (2 MHz). This effect of power transmission over changing frequencies is probably related to a wave length and skin effect [28][33].

Tx with 1MHz (resonant frequency) has 300 m of a wave length. This wave length is longer than 1.45 MHz (206 m) and 2 MHz (150 m). We guessed that the low resonant frequency is strongly coupled between Tx and Rx at a long distance. On the contrary, the high resonant frequency is loosely coupled between Tx and Rx at a long distance. This is one reason why the voltages (1 MHz) are higher than other conditions (1.45 MHz and 2 MHz).

The other reason is probably the skin effect. The skin effect makes Tx resistance to increase due to an eddy current. By increasing with alternating current, the eddy current increases arising from a changing magnetic field in the Tx conductor. It cancels the current flow in the center of the conductor came from power source. This tendency is certainly shown at a high frequency domain. So, the resistance of 1 MHz in the Tx is lower than the other frequencies (1.45 MHz and 2 MHz). The low resistance induces the strong alternating current in the Tx and it makes strong magnetic field in the channel. This is the other reason why the Tx with 1 MHz is better efficiency of power transmission compared with 1.45 MHz and 2 MHz.

3.4.5 Matching a resonant frequency at Rx

Previous experiments were processed under matching a resonant frequency at Tx. These were insufficient to enhance power transmission between Tx and Rx. So, it needs tuning conditions at Rx (1 mm 1 turn with MC). Rx antenna has low inductance value about 13 nH. To match a resonant frequency, Rx is connected to a capacitor with a high capacitance value in series model. Figure 3.3.4 shows the efficiency of matching resonant frequency at Rx. The conditions of Tx were same to 3.4.3 experiment. Only the resonance frequency was changed into 1.45 MHz. To match same resonant frequency

(1.45 MHz) both Tx and Rx, the capacitor with 1uF was connected at Rx in series model. The voltages were checked at Rx.

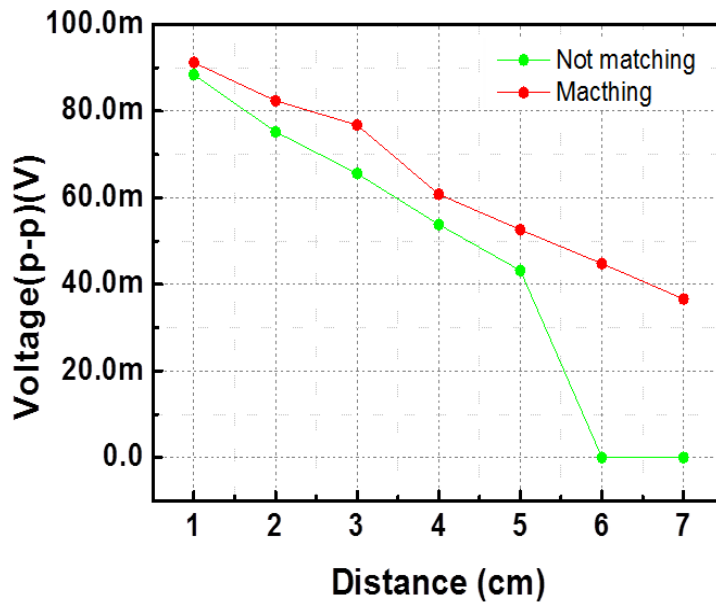


Fig 3.4.5 The matching effect of a resonant frequency at Rx

The red line and green show the efficiency of matching resonant frequency or not at Rx. The measured voltages of red line (matching resonant frequency at Rx) are higher than green line (not matching resonant frequency at Rx) over whole distance areas. Even the distances at 6 cm and 7 cm, the voltages (green line) were not checked. Matching resonant frequency both Tx and Rx, it can enhance the magnetic coupling and it makes a better efficiency of power transmission.

IV. CONCLUSION

We have studied the magnetic induction (MI) antenna structure for the power and the communication signal transmission to implanted devices inside the human body. To enhance the magnetic inductance, a three dimensional magnetic core was added to the flat spiral coil antenna structure, which was consisted of ZnO nano wires coated by the nickel (Ni) layer. ZnO nano wires supply easily a large effective surface area with a vertical structural effect to the magnetic core (MC) structure, which induces a higher magnetic fluxes with the ferro-magnetic material Ni. In the case of the MI antenna with MC, the inductance value (13.9 nH) is higher than without MC (11.5 nH) at 1 MHz. Reducing the outer diameter under 1 mm, the inductance values are higher than without MC cases. Considering the power transmission, the MI antenna with the MC showed a similar efficiency of power transmission at the water compared with the air medium. For the water medium and matching resonant frequency (2 MHz) only at Tx, the test used by 1 mm antenna with the MC structure (800 μm) shows the inductance value (64 mV) is the higher than without MC (57 mV) at 1 cm. Over increasing with distances from 1 cm to 8 cm, the measured voltages reduce both the coil with MC and the coil without MC. However, the coil with MC has high voltages over whole distances comparing with the coil without MC. The matching a resonant frequency and impedance between Tx and Rx are also important for wireless power transmission. When the Tx and Rx match a resonant frequency (1.45 MHz) and impedance (50Ω), the checked voltage is 91 mV at 1 cm. It is higher than not matching resonant frequency at Rx (64 mV). Therefore, this study shows a probability of the substitution to a traditional wire connection for the implanted systems.

References

- [1] S. Kim, O. Scholz, K. Zoschke., and M. Toepper. "FEA Simulation of Thin Film Coils to PowerWireless Neural Interfaces." *Nanotech 2006*, Vol. 1, 2006.
- [2] M. Topper, M. Klein, M. Buschick. "Biocompatible Hybrid Flip Chip Microsystem Integration for next Generation Wireless Neural Interfaces." *2006 Electronic Components and Technology Conference*, IEEE, 2006.
- [3] Thomas S. Rau, Andreas Hussong, Martin Leinung, Thomas Lenarz., and Omid Majdani. "Automated insertion of preformed cochlear implant electrodes: evaluation of curling behavior and insertion forces on an artificial cochlear model." *Springer*, 2009, pp. 173-181.
- [4] Eiichi Funatsu, Yoshikazu Nitta, Takashi Toyoda, Jun Ohta, and Kazuo Kyuma. "An Artificial Retina Chip with Current-Mode Focal Plane Image Processing Functions.", *IEEE Transactions on electron devices*, Vol. 44. 1997.
- [5] R. Bosshard, J. Muhletharler, J. W. Kolar, and I. Stevanovic. "Optimized Magnetic Design for Inductive Power Transfer Coils." *28th Applied Power Electronics Conference and Exposition*, Long Beach, California, USA, 2013.
- [6] David K. Cheng. *Field and Wave Electromagnetics*, Addison-Wesley, 1989, 703 pages.
- [7] Qiang Wang and Hong Li. "Research on the wireless power transmission system based on coupled magnetic resonances." *2011 International Conference on Electronics Communications and Control (ICECC)*, 2011.
- [8] Andre Kurs, Aristeidis Karalis, Robert Moffatt, J. D. Joannopoulos, Peter Fisher, and MarinSoljacic. "Wireless Power Transfer via Strongly Coupled Magnetic Resonances." *Science*, Vol 317, 2007.
- [9] Jianbo Gao. "Inductive Power Transmission for Untethered Micro-Robots." *31st Annual Conference of IEEE*, 2005.
- [10] J. Touminen. "Wireless power transmission." USA paten, No. 20012062[20030075670], 2003.
- [11] R. Krishnan. "Method and apparatus for wireless powering and recharging." USA paten, No. (6127799), 2000.
- [12] Zhi Sun and Ian F. Akyildiz. "Magnetic Induction Communications for Wireless Underground Sensor Networks." *IEEE Transactions on Antennas and propagation*, Vol. 58, No. 7. 2010.
- [13] <http://en.wikipedia.org/wiki/Solenoid>
- [14] Jonsener Zhao. "A new calculation for designing multilayer planar spiral inductors", Vol. 55, 2010, pp 37.

- [15] Peters, Christian, and Yiannos Manoli. "Inductance calculation of planar multi-layer and multi-wire coils: An analytical approach." *Sensors and Actuators A: Physical* 145, 2008, pp. 394-404.
- [16] Elias Haddad, Christina Martin, Bruno Allard, Maher Soueidan, and Charles Joubert. "Micro-fabrication of Planar Inductors for High Frequency DC-DC Power Converters." *Edited by Leszek Malkinski*, 2012.
- [17] S. Kim, K. Buschick, K. Zoschke, and M. Klein. "Polymer based thin film coils as a power module of wireless neural interfaces." *2006 IEEE Workshop on Microelectronics and Electron Devices*, 2006.
- [18] McLyman, Colonel Wm T. "Magnetic core selection for transformers and inductors." *Energy* 4. 1997.
- [19] Inoue, Shigenori, and Hirofumi Akagi. "A bi-directional isolated DC/DC converter as a core circuit of the next-generation medium-voltage power conversion system." *37th IEEE Power Electronics Specialists Conference*, 2006.
- [20] Yoon-Ki Sin, *Introduction to Electricity & Electronics*, Kyobobook, 2009.
- [21] Sugunan Abhilash, et al. "Zinc oxide nanowires in chemical bath on seeded substrates: role of hexamine." *Journal of Sol-Gel Science and Technology*, 2006, pp. 49-56.
- [22] Kim Hyunjin, et al. "Enhancement of piezoelectricity via electrostatic effects on a textile platform." *Energy & Environmental Science*, 2012, pp. 8932-8936.
- [23] Jung Inn Sohn, et al. "Engineering of efficiency limiting free carriers and an interfacial energy barrier for an enhancing piezoelectric generation." *Energy & Environmental Science*, 2013, pp. 97-104.
- [24] Wang, Zhong Lin. "ZnO nanowire and nanobelt platform for nanotechnology." *Materials Science and Engineering: R: Reports*, 2009, pp. 33-71.
- [25] Pospisilik, M, Kouril L, Motyl I, and Adamek. M. "Single and double layer spiral planar inductors optimisation with the aid of self-organising migrating algorithm." *In Proceedings of the 11th WSEAS international conference on Signal processing*, 2011, pp. 272-277.
- [26] Sunderarajan S. Mohan, Maria del Mar Hershenson, Stephen P. Boyd, and Thomas H. Lee. "Simple accurate expressions for planar spiral inductances." *IEEE Journal of Solid-State Circuits*, 1999, pp.1419-1424.
- [27] David C. Ng, Clive Boyd, Shun Bai, Gordana Felic, Mark Halpern, and Efstratios Skafidas. "High-Q flexible spiral inductive coils." *In Electromagnetic Compatibility Symposium-Melbourne*, 2010, pp. 1-4.
- [28] Yipeng Su, Chi Kwan Lee, and S. Y. (Ron) Hui. "On the relationship of Quality Factor and Hollow Winding Structure of Coreless Printed Spiral Winding (CPSW) Inductor." *IEEE Transactions on power electronics*, Vol. 27, 2012.
- [29] Xu, Sheng, et al. "Patterned growth of vertically aligned ZnO nanowire arrays on inorganic substrates at low temperature without catalyst." *Journal of the American Chemical Society*, 2008.

[30] Seung Nam Cha, et al. "Sound-Driven Piezoelectric Nanowire-Based Nanogenerators." *Advanced Materials*, 2010.

[31] Bedogni, G., et al. "Original communication accuracy of an eight-point tactile-electrode impedance method in the assessment of total body water." *European journal of clinical nutrition*, 2002.

[32] http://en.wikipedia.org/wiki/Impedance_matching

[33] <http://en.wikipedia.org/wiki/Wavelength>

요 약 문

나노기술을 활용한 인체삽입형 무선 임플란트 자기장 무선전력 송수신 시스템 연구

본 연구는 기존의 RF 방식이 아닌 자기장을 이용한 무선전력 송수신 및 통신 시스템개발을 다루고 있다. 일반적으로 통신 시스템에 사용되는 방식은 Radio Frequency (RF)를 주로 사용하였다. 하지만 RF 방식은 낮은 전력전송효율, 경로손실, 외부로부터 오는 잡음등과 같은 한계점으로 인하여 무선전력송수신 시스템에는 적합하지 않다. 또한 인체내부에 삽입되어 동작되는 인체삽입형 무선 임플란트에 RF 방식은 유해성을 가진다. 이러한 문제점들을 해결하기 위하여 본 연구에서는 자기유도를 활용한 무선전력송수신 방법을 제시하였다. 송신단과 수신단 사이에 자기 커플링을 활용하여 전력을 무선으로 전달할 수 있다. 자기장을 이용한 무선전력송수신 방법은 RF 방식에 비하여 인체에 무해하다는 장점을 가진다.

인체삽입형 무선 임플란트 시스템은 밀리미터 단위의 작은 사이즈를 가진다. 이에 맞추어 밀리미터 단위의 송수신 시스템 자기장 안테나 개발이 필요하였다. 공간의 소모성을 줄이기 위하여 평평한 나선 형태의 자기장 안테나를 다양한 턴 수, 외부직경을 가지도록 포토리소그래피, 리프트 오프 공정을 사용하여 제작하였다. 또한 보다 높은 전송 효율을 얻기 위하여 ZnO nano wire 를 활용하여 Magnetic Core 라는 자심을 안테나의 중심에 적용시켰다. 자심은 높은 투자율을 가지는 니켈을 ZnO nano wire 겹면에 스퍼터링 기술을 활용하여 덮었다. 자심 구조체는 외부로 손실되는 자기장영역을 안테나의 중심으로 집중하게 만드는 역할을 한다. 자심 구조체를 적용한 마이크로사이즈 자기장 안테나의 인덕턴스값을 자심 구조체를 적용하지 않은 마이크로사이즈 자기장 안테나와 비교하였다. 자심 구조체를 적용한 자기장 안테나의 경우의 인덕턴스 값이 자심 구조체를 적용하지 않은 경우보다 높은 값을 가졌다.

무선 전력송수신 효율을 파악하기 위하여 공기중과 인체와 유사한 수중에서 실험하였다. 공기중과 수중에서 자기장을 이용한 무선전력송수신 효율은 비슷하였으며, 자심 구조체를 적용한 마이크로사이즈 자기장 안테나가 높은 무선전력송수신 효율을 보였다.

본 연구는 차세대 인체삽입형 무선 임플란트 기술에 핵심부분이 될 무선전력송수신을 실험하여 앞으로의 방향을 제시해주었다는 점에 대해서 의의를 가진다.

핵심어: 자기장, 자심, 나노 와이어

감사의 글

벌써 대구경북과학기술원에 입학한지 2 년이 다되어 갑니다. 황무지였던 들판에 도로, 아파트, 건물들이 들어서는 과정을 보고 느끼면서, 제 자신이 변화하는 모습도 보게 되었습니다. 아무것도 모르는 철부지였던 학생에서 자신의 분야에서 목소리를 낼 수 있는 전문인이 되어왔습니다. 짧지만 많은 2 년이라는 기간 동안 제가 이 자리에 설 수 있기까지 주변에 많은 고마우신 분들이 있었습니다. 고마운 마음을 글이나마 표현하기 위해서 이렇게 감사의 글을 몇 글자 적어 봅니다.

저의 역량을 최대한 이끌어내기 위해서 연구에 관한 조언을 언제 어디서나 해주셨고, 연구자로서의 자세에 대하여 지도해주신 장재은 지도교수님 정말 감사합니다. 연구, 대학원 생활, 진학관련 어려움에 빠져있을 때 격려의 한 말씀은 제가 올바른 길을 갈 수 있도록 하는 원동력이었습니다. 지도교수님과 함께 학위논문을 공동으로 지도해주신 신 물질과학과 홍정일 교수님, 정보통신융합과 통신 연구실 최지웅 교수님 감사합니다. 물질과 통신관련 아이디어를 교수님들의 조언으로 얻을 수 있었고, 학위논문을 더욱더 알차게 작성할 수 있었습니다. 또한, 진심어린 마음으로 해주신 권옥현 석좌교수님, 손상혁 전공책임교수님, 박태준 교수님, 은용순 교수님, 박경준 교수님, 김민수 교수님, 최지환 교수님 감사합니다.

Advanced Electronic Devices Research Group (AEDRG) 에 속해 있으면서 즐겁게 생활할 수 있도록 도와주신 선배님, 후배님들에게도 감사의 말을 전합니다. 지금은 공항공사에서 활기차게 업무에 열중하고 있는 임재한 선배님, 교수님의 오른팔 신정희 선배님, 삶의 조언을 많이 해주신 이광준 형님, 2 년동안 재미있게 웃고 서로 도와가며 힘든 시절을 이겨 낼 수 있도록 도와준 김승욱, 정예리 동기님, 연구실에서 가장 잘생긴 전병욱 형님, 그래핀 연구의 선두주자 양재훈님, 교수님의 왼팔이 될 심민경 후배님 감사합니다. 또한, 3기 동기, 학과 선배, 후배님들에게도 감사의 글을 전합니다.

마지막으로 제가 이 자리에 있기 까지 저를 믿어주시고 응원해주신 저의 부모님, 형제들에게 감사의 말을 전합니다. 성실한 자세를 강조하셨고 실천하라고 말씀해주신 아버지, 주변분들에게 항상 감사하며 보답하라고 말씀해주신 어머니, 저를 열심히 응원하고 도와준 누나, 형을 믿어주고 자신감을 가질 수 있도록 해준 동생 정말 감사합니다. 비록 글로써 언급하지 않았지만 제 주변분들에게도 감사의 말을 전합니다. 감사합니다.